

Copyright

by

Jeffrey James Mitchell

1995

**CORROSION PERFORMANCE OF A SECOND-GENERATION HIGH
RATIO ZINC SILICATE COATING IN A REINFORCED CONCRETE
ENVIRONMENT**

by

JEFFREY JAMES MITCHELL, B.S.E.

THESIS

Presented to the Faculty of the Graduate School

of The University of Texas at Austin

in Partial Fulfillment

of the Requirements

For the Degree of

MASTER OF SCIENCE IN ENGINEERING

The University of Texas at Austin

May, 1995

**CORROSION PERFORMANCE OF A SECOND-GENERATION HIGH
RATIO ZINC SILICATE COATING IN A REINFORCED CONCRETE
ENVIRONMENT**

APPROVED BY:

Dr. James O. Jirsa

Dr. Ramon L. Carrasquillo

To Gina Kay, and to my Family

With Love and Thankfulness

ACKNOWLEDGMENTS

I would like to acknowledge all those who contributed to this work, for although it was an individual project, it was certainly not done alone. First, I would like to thank Dr. James O. Jirsa for his excellent supervision and guidance. I am thankful to have worked with a professor of such caliber. I would also like to thank Dr. Ramon L. Carrasquillo for his editorial comments during the writing process.

A number of colleagues at Ferguson Laboratory were instrumental to the set-up and maintenance of the project. Previous work conducted by Robert Frosch and Khaled Kahhaleh was foundational to this research, and Enrique Vaca was very kind to offer comments and take readings on many occasions. I would like to express my sincere appreciation to Hasan Pasha, who also helped with readings and performed countless chloride tests with great efficiency.

Finally, I would like to thank the laboratory and office staff at Ferguson for their patience, assistance, and humor, and Inorganic Coatings, Inc., for providing the necessary funding. It was a pleasure to work with all of you.

Jeffrey James Mitchell

December 13, 1994

ABSTRACT

CORROSION PERFORMANCE OF A SECOND-GENERATION HIGH RATIO ZINC SILICATE COATING IN A REINFORCED CONCRETE ENVIRONMENT

by

Jeffrey James Mitchell, M.S.E

The University of Texas at Austin, 1995

SUPERVISOR: James O. Jirsa

The macrocell method was used to evaluate a high ratio zinc silicate coating for corrosion performance on concrete reinforcing steel. Twenty-seven macrocells were constructed and subjected to cyclical chloride exposure for 364 days. The variables investigated were the effects of coating damage, the effects of coating the cathode steel, and two repair techniques. As a comparison, galvanized steel was used in six of the specimens, and epoxy-coated steel was used in three specimens.

It was found that the zinc silicate coating provided good corrosion protection throughout the 364 days of exposure when the coating was applied to all the steel. Substantial levels of corrosion were observed when only some of the steel was coated. The zinc silicate coating performed significantly better than the galvanized coating, although less corrosion was observed on the epoxy specimens than on the zinc silicate specimens due to the excellent initial condition of the epoxy coating.

TABLE OF CONTENTS

	Page
CHAPTER 1: INTRODUCTION	1
1.1 Background	1
1.2 Objectives	3
1.3 Scope	4
1.4 Analysis of Results	5
CHAPTER 2: BACKGROUND TO THE CORROSION OF STEEL IN CONCRETE	 6
2.1 Mechanism of General Corrosion	6
2.2 The Effect of Passivation	10
2.3 The Chloride Effect: Corrosion of Steel in Concrete	11
2.4 Galvanic Corrosion	15
2.5 Corrosion Protection for Steel in Concrete	18
CHAPTER 3: THE USE OF ZINC FOR CORROSION CONTROL IN CONCRETE	 24
3.1 Zinc Corrosion Properties	24
3.2 Methods of Application	27
3.3 Inorganic Zinc Coatings	28
3.4 Concluding Considerations: Zinc in Concrete	33

CHAPTER 4: EXPERIMENTAL THEORY AND PROCEDURES	35
4.1 The Macrocell Method	35
4.2 Experimental Variables	42
4.3 Condition of Steel Prior to Concrete Placement	45
4.4 Chloride Specimens and Tests	53
4.5 Construction of Formwork and Steel Placement	54
4.6 Concrete Placement	57
4.7 Sample Preparation	58
4.8 Evaluation of Macrocells	60
4.9 Procedural Modifications	62
 CHAPTER 5: TEST RESULTS	 63
5.1 Introduction	63
5.2 Corrosion Current Data	63
5.3 Charge Flow Data	72
5.4 Inspection After Seven Months of Exposure	80
5.5 Inspection After Thirteen Months of Exposure	87
5.6 Corrosion Products	100
5.7 Chloride Data	101
 CHAPTER 6: SUMMARY, CONCLUSIONS AND RECOMMENDATIONS	 105
6.1 Summary	105

6.2	Conclusions	107
6.3	Recommendations	109
	BIBLIOGRAPHY	110
	VITA	113

CHAPTER 1

INTRODUCTION

1.1 Background

The problem of steel corrosion in concrete is a significant issue facing the construction industry today. The corrosion of reinforcing bars affects an enormous number of bridges, roadways, and parking garages in northern regions, as well as many coastal structures. In one study,^[26] twenty-two bridge decks were visually inspected, and 40% of the decks containing untreated reinforcing bars were in the initial stages of deterioration. In another investigation,^[3] 249 bridges were inspected. Twenty-five percent of the decks showed potholes and fracture patterns indicative of corrosion. None of the 249 bridges had been through more than four winter seasons. Clearly, corrosion is a major problem in reinforced concrete structures and merits extensive attention.

Corrosion damage manifests itself in the form of progressive deterioration. As the steel corrodes, chemical products are produced that take up more than twice the volume of the original material. The volume increase around the bars creates expansive pressures on the order of 5000 psi. Cracks then begin to form in the concrete, allowing additional corrosive agents to gain access to the steel and accelerating deterioration. Fracture planes form, rust-colored stains appear on the surface of the concrete, larger pieces of concrete begin to spall away, and the structure becomes unserviceable. These problems are alarmingly acute in places where deicing salts are applied to roadways and in marine environments (particularly in the splash zones).

Although there are numerous corrosion mechanisms that may occur, the overall process can be summarized quite simply. There must be a liquid environment, a material to be corroded, and a catalyst that consumes electrons. In the case of steel in concrete, water, oxygen, steel, and chloride ions usually provide the necessary ingredients. In a typical corrosion cell, water, oxygen and chloride ions diffuse into the concrete to the depth of the reinforcing steel. The chloride ions depassivate the steel, iron atoms dissolve into solution, electrons are liberated, oxygen consumes the electrons by forming OH^- , and the dissolved iron ions recombine to form corrosion products, such as Fe_3O_4 and Fe_2O_3 . This process requires that water, steel, oxygen, and chloride ions all be present in the concrete; the corrosion of steel in concrete will almost never take place in the absence of any one of these materials, unless carbonation or cracking produces a change in the pH of the pore water.

A number of different corrosion protection systems have been developed to curtail the corrosion of steel in concrete. Traditional protection schemes include the use of high-quality concrete and adequate cover, the installation of water and ion barriers, impressed cathodic current, and the coating of the reinforcing steel. The work reported here focuses on sacrificial coatings for reinforcing steel.

One type of coating system uses an electrochemically active metal - typically zinc - to coat the steel. The zinc coatings both provide a barrier against water and chlorides and galvanically protect the steel surface. Zinc is used primarily for economic reasons, as zinc is cheaper than magnesium and other sacrificial metals. Zinc also remains passive to lower pH's than steel, and is several times more resistant than steel to corrosion in the presence of chlorides.

Zinc may either be applied to steel in the form of hot-dip galvanizing, or in the form a zinc-based paint. Considerable research has been done in the last 50

years in the development of zinc-based paints. The latest zinc coatings, the high ratio inorganic zinc silicates, are an outgrowth of NASA technology, devised to protect rocket launchers from corrosion.

The high ratio zinc silicates are water-based and self-curing, combining the simplicity of one coat with the environmental benefits of a water-based solvent, instead of a VOC-based solvent (volatile organic compound).^[19] The zinc silicates function by binding metallic zinc to the steel surface in an inorganic polymer matrix. After curing, the coating is hard, insoluble, and can be recoated. The presence of zinc in the coating provides a measure of galvanic protection for the steel. Exposure tests have demonstrated this protection over the last 14 years in severe chloride environments.

It remains to be demonstrated, however, that the high ratio zinc silicate coatings will perform well in a high pH, resistive, concrete environment. This report deals with research conducted at the University of Texas at Austin to investigate the use of high ratio zinc silicates in reinforced concrete for the control of reinforcing steel corrosion.

1.2 Objectives

A series of experiments were designed to examine the corrosion behavior of a specific high ratio zinc silicate coating in a concrete environment. Previous tests carried out at the University of Texas at Austin found that a "first-generation" zinc silicate coating did not provide effective corrosion protection.^[12] The goal of the present experiments is to determine whether a reformulated (second-generation) coating shows an improvement over the previous coating, and whether the

improvement is substantial enough to make the new formulation a viable product for reducing the corrosion of steel in concrete.

1.3 Scope

The experiments reported here closely followed the same procedures used to evaluate the first formulation. The macrocell method was used to monitor corrosion behavior in a forced corrosion environment. The macrocells consisted of blocks of concrete cast with fixed amounts of steel in top and bottom mats. Instrumentation was set up to weekly monitor the potential differences between the steel layers.

Salt solution was ponded on the top of the macrocells in 14-day, wet/dry cycles. The top steel became exposed to chlorides in solution and was forced to become the anode in an electrochemical corrosion cell. Electrons liberated at the anode traveled through a conductor to the bottom layer of steel, producing the corrosion currents that were monitored.

Separate concrete chloride cells were also constructed and subjected to the same exposure cycle in order to monitor the diffusion of chloride ions into the concrete. Drilled samples of concrete dust were taken from specified depths on a monthly basis and analyzed for chloride concentration.

Nine different coating combinations were used on the steel. The primary coating variables investigated were the effects of damage to the high ratio zinc silicate coating prior to concrete placement, the effectiveness of two different repair techniques, and the effects of using coated, rather than uncoated cathodes.

1.4 Analysis of Results

The macrocells provided three types of data for analysis. First, the potential difference readings were used to calculate instantaneous corrosion current and charge flux magnitudes. Corrosion current vs. time plots were developed to illustrate the theoretical corrosion activity in the macrocells throughout the experiment, and charge flux vs. time plots were created to show the theoretical cumulative damage levels.

Second, the theoretical data were compared with visual observation of the corrosion damage. Macrocells were opened on two occasions, permitting corrosion damage levels and locations to be photographed and described.

Finally, chloride concentration depth profiles from the chloride cells were examined over time and compared to concentration profiles obtained from the macrocells during the autopsies. These data allowed the penetration of the chlorides into the concrete to be monitored for magnitude and consistency.

CHAPTER 2

BACKGROUND TO THE CORROSION OF STEEL IN CONCRETE

2.1 Mechanism of General Corrosion

Corrosion is an electrochemical process requiring two reactions - the anodic and cathodic reactions. These two reactions are sequential, but both must be present for the process of corrosion to be sustained.

The anodic reaction provides the electrons needed in the electrochemical process. A metal atom dissolves into solution as a positive ion, liberating one or more electrons. These electrons then travel through the material by conduction to the location of the cathodic reaction. The distance of travel for the electrons may be extremely small (on the order of microns), or comparatively large (on the order of meters).

At the cathode, a second reaction takes place that consumes the electrons provided by the anodic reaction. An aqueous, ionic species combines with electrons on the surface of the conductor to form a new compound.

There are many possible forms of anodic and cathodic reactions. The anodic reaction is the simplest: metal atoms dissolve into solution. In the case of iron and steel, it is the iron atom that participates in this reaction. The reaction is given below:



Or, more generally, for the case of any metal, M:



The cathodic reaction can take a variety of forms. For example, in acidic environments, H^{+} ions in solution combine with free electrons to form hydrogen gas. In other environments, metal ions or metal ion complexes with high valence charges combine with electrons to form ions with lower valences. In the case of steel or iron in aqueous environments, dissolved oxygen and water molecules may also combine with free electrons to form OH^{-} ions in the reaction: ^[10]

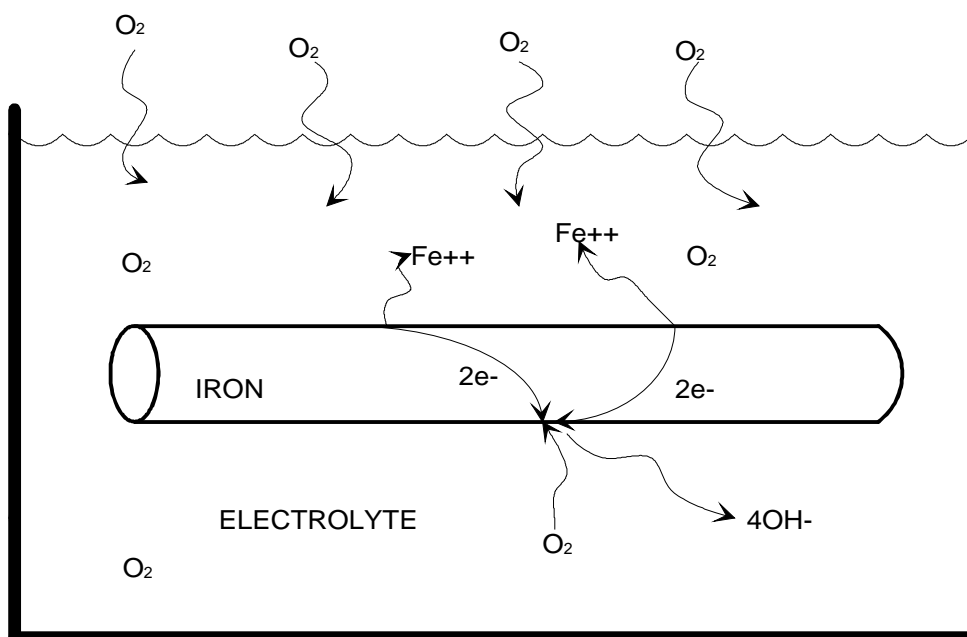


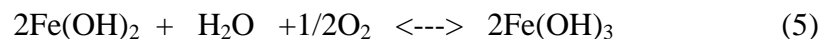
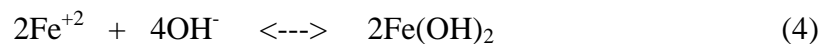
Figure 2.1: Anodic and Cathodic Reactions in the General Corrosion of Iron

Figure 2.1 illustrates this iron-oxygen-water chain of reactions, in which the iron corrodes to form Fe^{++} and the liberated electrons combine with water to

produce OH⁻. Hydroxide ions and aqueous iron ions are therefore the products of the anodic and cathodic reactions.

It is important to note that oxygen does not participate in the anodic reaction - oxygen is required only at the cathode to participate in the reduction described by formula 3. In fact, the presence of oxygen at the anode can obstruct corrosion by retarding the dissolution rate of iron by forming surface oxides. ^[9]

In addition to the anodic and cathodic reactions, subsequent reactions may take place involving the aqueous iron ions, producing the corrosion products commonly associated with rust. A possible chain of reactions is:



Three more factors must also be included in the discussion of general corrosion: the electrolyte, material resistance, and potential difference. First, there must be an electrolyte linking the anode and the cathode in order to sustain corrosion. The electrolyte provides the environment for the corrosion process by acting as the medium for ionic diffusion. Metal ions require a fluid environment for dissolution, and ionic corrosion products produced at the cathode must be able to diffuse back toward the anode. The electrolyte therefore provides the corrosion medium and the necessary link between the cathode and the anode.

The effectiveness of the electrolyte as a corrosion-facilitator is a strong function of the number of ions in solution. As ionic concentrations increase, corrosion rates also tend to increase. This effect stems from the fact that more corrosive species tend to be present in high concentration environments, and ionic

diffusion rates are increased. As a corollary to this phenomenon, the high concentration electrolytes have lower electrical resistance, further aiding corrosion.

The resistivity of the corroding material is also of great importance. The anodic and cathodic reactions do not take place in isolation; electrons produced at the anode must have a way to get to the site of the cathodic reaction. There must therefore be a path of electrical conductance between the anode and the cathode. If there is no link between the reaction sites, corrosion will not take place. For this reason, it is generally observed that substances that corrode are low-resistance materials.

A final piece in the puzzle of general corrosion is electrical potential. Electrical "force" is required to move the electrons generated at the anode to the cathode. This "force" is provided by a potential difference between the anode and cathode, with the anode at a greater negative potential. Potential differences may be caused by interaction between the environment and the material, metallurgical factors, or applied currents.^[11]

To summarize, several key ingredients must be present for general corrosion to occur. There must be corroding material capable of supplying electrons, a substance that desires to consume electrons, an electrolyte that brings the "electron-hungry" substance into contact with the corroding material, and a path of electric conductance between anodic and cathodic sites. In the case of steel and iron corrosion in aqueous environments, equations 1 and 3 describe the typical anodic and cathodic reactions. Equations 4 and 5 describe subsequent reactions that produce the commonly observed iron corrosion products.

2.2 The Effects of Passivation

The corrosion of many metals is also influenced by a phenomenon known as material passivation. Metals such as titanium, stainless steel, iron and carbon steels react to form surface oxides that retard or prevent the dissociation of metal ions into solution. Passivation takes place under environmental conditions that vary from metal to metal.

In the case of steel and iron, passivation occurs when a surface oxide of gamma iron forms. This passive layer is invisible and its composition has not been established exactly, except that it involves oxygen.^[9] Steel will not corrode while its passive layer remains intact. An important property of this passive layer is its instability in most environments except those of high pH. Steel and iron will depassivate in solutions of pH less than 10 or 11.

Most commonly encountered aqueous environments have fairly neutral pH's of about 7. Under such conditions, steel will not passivate. However, the pH in moist concrete is typically about 13, due to the presence of calcium hydroxide ($\text{Ca}(\text{OH})_2$), a by-product of hydration. Under normal conditions, therefore, steel will not corrode inside concrete. This environmentally-produced corrosion protection has been observed to be effective, except under certain circumstances.

Steel will only corrode in concrete environments if the pH is lowered below the 10.0 threshold, or if the passive layer is broken down in some other way. Carbonation will lower the pH of concrete pore water past the 10.0 limit, but the process takes considerable time. It is rare to see carbonation effects present in good quality, uncracked concrete below a depth of 1/2 in.^[5] Cracking and insufficient cover can make carbonation a threat.

Steel may also depassivate in high pH environments in the presence of bromide ions. The most commonly found bromide ion in concrete environments is chloride, and chloride does pose a very real threat to the integrity of many reinforced concrete structures.

2.3 The Chloride Effect: Corrosion of Steel in Concrete

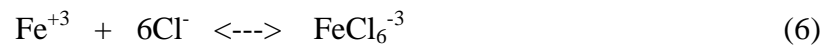
The chloride ion is a very common substance in many reinforced concrete environments. The most common source of solid chloride is salt (NaCl). In this form, chlorides come into contact with concrete through deicing applications, contaminated mix water, marine environments, and contaminated aggregates. Chloride ions are also introduced through the use of some accelerating admixtures, such as calcium chloride, and concrete bleaching operations.

In order to promote corrosion, free chloride ions must be present in moist concrete at the level of the reinforcing steel. Aqueous chloride ions may come into contact with the reinforcing steel as water saturates concrete that already contains chloride, or as dissolved chloride ions diffuse through the concrete mass. The diffusion of chloride ions from the outside of the concrete to the interior is the most common mechanism resulting in chloride exposure.

Chloride ions do the most damage when they enter reinforced concrete after hydration has stopped and the concrete has hardened. The process of hydration can remove up to approximately 7 g/l of chloride from fresh concrete.^[17] This removal takes place as aqueous chlorides react with tricalcium aluminate (C_3A), a compound in portland cement. However, the reaction between C_3A and chlorides is affected by several factors, and it is generally not wise to rely on hydration to remove significant amounts of chlorides. This is especially true when the chlorides are present after hydration has slowed.

Corrosion begins once free chloride and water are present at the surface of the steel in critical amounts. The precise mechanism of chloride-induced corrosion, however, is not known. There are at least five different theories as to why chlorides

induce corrosion. One body of research indicates that chloride ions promote corrosion by forming compounds that liberate iron ions from the steel surface. The small chloride ions are able to diffuse through the protective passive layer and combine with the steel to form chloride complexes.^[9] One possible reaction is:



The chloride-iron compounds produced then react with the abundant hydroxide ions in solution to produce the common steel corrosion product, $\text{Fe}(\text{OH})_2$. The predicted reaction is given below in equation 7:



Note that in the above reaction, the chloride ions are released to participate further in the corrosion process.

According to a second theory,^[9,15] corrosion is accelerated as the chloride-iron complexes hydrolyze to form hydrochloric acid. This theory is substantiated by the claim that pH's of 3.0 have been measured immediately adjacent to severely corroding reinforcing steel. Some researchers^[9] dismiss this claim, however, insisting that the substantial buffer of hydroxide ions in the concrete pore water will neutralize any H^+ ions produced by hydrolysis.

The final corrosion products produced by chloride corrosion vary with environment. Where sufficient oxygen is available, the common, rust-colored iron oxides may be expected. In low-oxygen environments, however, dark green and dark gray/black corrosion products have been observed on bare steel anode sites.^{[1,}

^{12]} It is postulated these products are chloride-iron complexes that fail to form iron

oxide due to the lack of oxygen. The dark green products often turn rust-colored in a matter of minutes when exposed to the atmosphere.

Regardless of the exact mechanism and by-products, it is universally accepted that chloride ions induce the corrosion of steel in concrete. When steel is exposed to aqueous chloride ions, the electrical potential of the steel becomes more negative, and anode sites are established.

It is important to note that water and chloride are not the only ingredients required for corrosion to occur. The water and chloride establish the anodes, but oxygen (or some other electron-consumer) and water must be present at the cathodes, and electrical and ionic conductivity must exist between the two sites. Chlorides simply act as catalysts where conditions for corrosion are favorable.

Figure 2.2, below, illustrates an example of a chloride-induced corrosion macrocell. Chlorides and water penetrate to the level of the top steel and establish the anode. Water saturates the concrete to the depth of the lower mat of steel, where oxygen is more available. Steel stirrups link the anodic top steel to the cathodic bottom steel, providing a pathway for the electrons. This scenario is common in bridge decks and other reinforced concrete surfaces exposed to deicing salts.

Microcell corrosion may also be induced by aqueous chlorides. In the case of microcells, variations in chloride ion concentrations place one area of steel in a higher electrical potential than an adjacent piece of steel. If sufficient oxygen is present, corrosion will proceed locally. Pitting corrosion is an example of local microcell action. Differentials in chloride ion concentrations thus become very important - often more important than the absolute magnitude of the overall chloride ion concentration. ^[1]

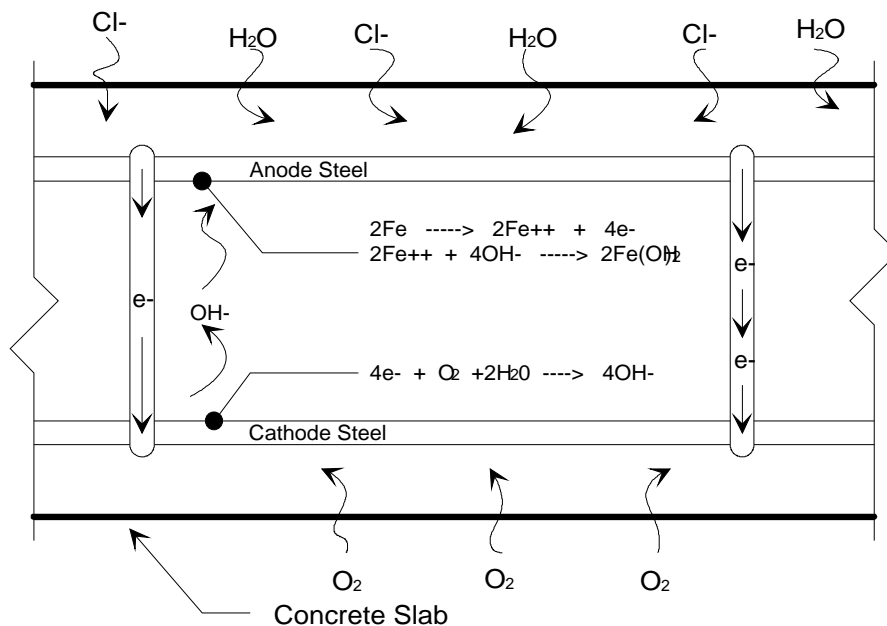


Figure 2.2: Chloride-Induced Macrocell Corrosion

The corrosion of steel in concrete is often self-accelerating, leading to progressive deterioration. The products of steel corrosion occupy more than 2 times the volume of the original materials. This increase in volume can create internal expansive pressures of approximately 5000 psi, causing the concrete to crack. Cracks in the concrete then allow more water, chlorides, and oxygen to reach the level of the steel, and the corrosion rate increases. It is very common to find severe reinforcing steel corrosion - particularly pitting - at the site of cracks.

As corrosion progresses, cracks become wider and more numerous. Corrosion products are forced to the surface and unsightly staining of the concrete may be observed. In the later stages of corrosion, pieces of concrete may spall away from the surface. This is often referred to as "potholing". Costly repairs then become necessary. In some instances, the structures may need to be demolished.

The problem of chlorides in reinforced concrete structures is therefore a significant one. Chlorides promote corrosion and have been instrumental in the damage and decay of many concrete structures. Billions of dollars in corrosion damage have already been realized, and more is likely in the future. It is the goal of many researchers to find a way to prevent chlorides from taking part in the process of steel corrosion in concrete environments.

2.4 Galvanic Corrosion

The topic of galvanic corrosion is worthy of discussion because it provides a theoretical basis for at least one solution to the problem of steel corrosion in concrete.

Galvanic corrosion is the name given to the phenomenon of coupled corrosion. Conductive materials may be classified in terms of their potentials with respect to a standard hydrogen electrode, or their standard emf. Metals may additionally be classified in terms of their potentials in other environments, such as seawater. When two metals are dissimilar, as determined by their location in the emf or comparable series, and are connected electrically and placed in a conductive, corrosive environment, it is generally observed that one metal experiences accelerated corrosion, while the other metal experiences less corrosion than if placed in the same environment, alone and uncoupled.^[10] This change in corrosion behavior is a direct result of the potential difference that exists between the two metals in the corrosive environment. The metal with the more negative potential becomes the anode, and the metal with the less negative potential with respect to the standard electrode becomes the cathode. In some cases, the cathode, or protected metal, may demonstrate little or no corrosion.

Several points must be emphasized with respect to galvanic corrosion. A good electrical contact must exist between the two coupled metals, the environment must be a conductive solution, and both metals must be in contact with the environment. If the electrical contact between the metals is poor, or if the environment is highly resistive, galvanic action will not take place as strongly.^[25] Also, if only one of the metals is subjected to the environment, that metal will corrode as if it were uncoupled in that environment.

Additionally, galvanic couples are environment-specific. Two metals that show definite galvanic action in one environment may show little or no galvanic corrosion in other environments. In some cases, the relationship between the metals may even reverse; a metal that is cathodic to another metal in one environment may become anodic to the same metal in another environment. This behavior is directly a function of the relative potentials of the coupled metals in the specific surroundings.^[10]

Finally, the presence of a passive layer on the metal may complicate analysis. Certain metals may become more passive when subjected to higher corrosion potentials. This is not the case with steel in most environments, however.

The concept of galvanic corrosion has been used in a number of protection schemes for steel, with galvanizing as probably the most common technique. In galvanizing, steel is dipped in molten zinc, forming an outer coating of zinc and zinc alloys on the steel. Zinc coatings protect the steel by providing both a barrier and galvanic protection; where a break occurs in the zinc and both zinc and steel become exposed to corrosive attack, the zinc corrodes preferentially to the steel. Galvanic action takes place because zinc is more electrochemically active than steel in most environments. Figure 2.3, below, illustrates the concept of galvanic protection. As shown, the corrosion rate of the zinc in the vicinity of a break in the coating accelerates, protecting the iron even in the absence of the barrier.

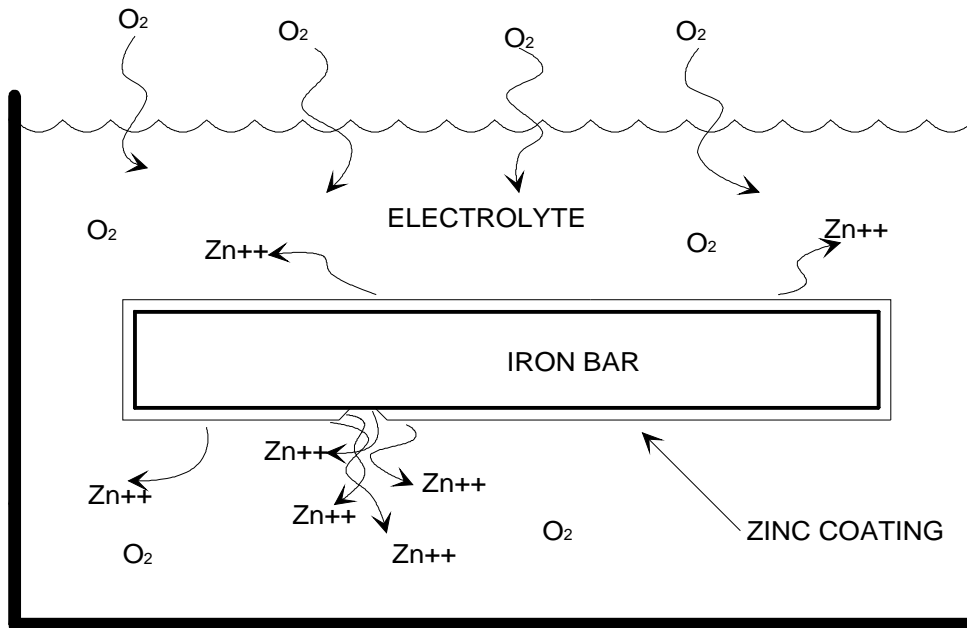


Figure 2.3: Sacrificial Action in a Galvanic Couple

2.5 Corrosion Protection for Steel in Concrete

A number of different approaches to preventing steel corrosion in concrete have been developed and refined in recent years. The most significant of these schemes include exposure reduction, the use of corrosion inhibitors, cathodic protection, and the use of reinforcing steel coatings. Each of these methods will be briefly described below.

2.5.1 Exposure Reduction

Exposure reduction is the simplest (and some would say, most effective) method of corrosion reduction. By preventing chlorides, water, and oxygen from reaching the reinforcing steel, corrosion becomes impossible. Exposure reduction can first be achieved by placing the concrete in an environment free from dangerous substances. This is not a practical option, however, as concrete placed outside will become exposed to water and oxygen, and structures located in marine or snow-belt areas will be exposed to chloride ions. The only remaining possibility consists of preventing the harmful materials from diffusing into the concrete.

Concrete permeability and adequate cover are the key variables in preventing this diffusion. Concrete with lower water permeability will obviously show lower chloride diffusion rates. Oxygen and ionic diffusion rates will similarly be retarded. Increased cover over the reinforcing steel will always provide additional corrosion resistance.

Concretes with lower permeability also show substantially higher electrical resistivity than more permeable concretes. This reduces the speed at which corrosion may take place, regardless of the chloride ion concentration. Indeed, some engineers claim that increasing concrete resistivity and excluding oxygen are the most significant and trustworthy methods of corrosion prevention.^[1,11]

There are a number of ways to obtain low permeability concrete. The simplest involves using good concrete; properly placed, well consolidated, and correctly finished concrete designed with a low water/cement ratio (.45 or less) and cured properly will have a low permeability.

Other methods of reducing permeability involve the use of admixtures or special materials. Latex modifiers, polymer compounds, and silica fume are examples of concrete additives that lower the permeability. The use of special additives may be too costly, however.

Finally, impermeable membranes may be placed within the concrete between the reinforcing steel and the source of corrosive agents. Sealing compounds may also be applied to exposed surfaces. Both of these methods have shown some success in selectively lowering concrete permeability and delaying the onset of corrosion. ^[3]

All of the above methods have shown some practical success. The water/cement ratio is probably the most widely-acknowledged method in permeability reduction. None of these methods, however, can completely prevent corrosion once the chlorides, oxygen, and water become present in the concrete in sufficient amounts.

2.5.2 Corrosion Inhibitors

Corrosion inhibitors provide a method (in theory) to stop the corrosion process even though all necessary ingredients for corrosion are present. An inhibitor is a substance that acts as a "reverse catalyst" that slows or stops the corrosion rate. Most inhibitors are proprietary and empirically developed, so little is known about the exact mechanisms and reactions involved. It is known, though, that inhibitors tend to function in one of several modes.

The first class of inhibitors function by adsorption. These inhibitors first diffuse into and bond with the surface of the metal subject to corrosion. The adsorbed inhibitors then function as a form of applied passivation by obstructing the anodic and cathodic reactions. Adsorption inhibitors account for the majority of corrosion inhibitors used. ^[10]

A second class of inhibitors contain hydrogen-evolution poisons. These inhibitors function by specifically targeting the hydrogen reduction reaction:



The hydrogen poisons reduce the corrosion rate by retarding the cathodic reaction found in acidic environments. These inhibitors are not useful in basic environments such as concrete, where oxygen reduction provides the cathodic reaction.

A final class of corrosion inhibitors is the oxidizers. Oxidizers prevent the corrosion of metals (such as steel) that exhibit active/passive transitions. These inhibitors perform by stabilizing the passive layer, retarding the anodic corrosion reaction.

In general, the use of corrosion inhibitors has seen only limited success. Inhibitors are designed to target very specific reactions, in a very specific range of concentrations. When additional reactions come into play, or when the concentration of corrosive agents changes, corrosion inhibitors quickly lose their effectiveness. In addition, a number of inhibitors are toxic, and can be used only with great care where the consequences of contamination are severe. Corrosion inhibitors therefore present, at best, only a partial solution to the problem of corrosion in concrete.

2.5.3 Cathodic Protection

Cathodic protection, in various forms, has been used for quite some time. This method of corrosion protection works by extinguishing the potential differences that drive the corrosion process. Cathodic protection applies an equal and opposite potential, in the form of impressed electrical current, between the anode and cathode in the corrosion cell. When the potential difference is thus externally forced to zero, corrosion stops. Corrosion cannot occur when cathodic protection is properly applied and maintained.

The current demand in most typical cathodic protection applications is not very large. A fraction of a milliampere is usually all that is required per square foot

of concrete surface. Protection for 10,000 square feet of concrete would draw about as much power as a 150 watt light bulb. ^[15]

A number of different methods can be used to implement cathodic protection in reinforced concrete. Conductors may be installed on the surface of a concrete slab, under concrete overlays, or on the surface of the reinforcing steel. Alternatively, conductive concrete overlays may be used to conduct the impressed current.

DC potentials opposite in sign to the anticipated corrosion cells are then applied to the concrete from a dedicated power supply unit. All cathodic protection schemes involve the use of a controlled current through the concrete mass.

Although often very effective, cathodic protection does present several problems. First, cathodic protection is not possible unless the anodes and cathodes can be absolutely identified. If current of the incorrect sign or magnitude is applied, the steel corrosion can be accelerated, with disastrous results. Cathodic protection is therefore only possible where macrocell corrosion is anticipated.

Second, cathodic protection schemes may cause peripheral corrosion problems. Metal appurtenances, ducts, and conduits may be induced to corrode by stray DC currents. Steel in contact with the concrete must be carefully isolated.

Cathodic protection is therefore not the solution to every concrete corrosion problem. It has been used successfully, though, in a number of applications, including many bridge decks.

2.5.4 Direct Coating of Reinforcing steel

A final corrosion protection scheme for steel in concrete involves directly coating the reinforcing steel. Two types of coatings are currently used: simple barrier coatings, and sacrificial coatings. Epoxy barrier coatings are produced by fusion-bonding an epoxy-based powder with the surface of the steel. The epoxy

coating forms a barrier that prevents water and chloride ions from reaching the surface of the reinforcing steel. As barriers, epoxy coatings are only beneficial when the integrity of the coating remains good. Breaks in the epoxy caused by handling or poor application processes allow corrosion to take place in localized areas. Furthermore, such localized corrosion can become very severe due to small anode/cathode area ratios.

This shortcoming is exaggerated by the fact that epoxy coatings are comparatively soft, and damage is virtually inevitable. When epoxy coatings were first used, proponents predicted corrosion protection in excess of 20 years. Current estimates indicate corrosion protection of 10 years or less. While the corrosion benefits of epoxy coating cannot be denied, lower-than-expected field performance and problems with bond strength have caused a number of users investigate other protection options.

Galvanic coatings, on the other hand, provide both a barrier to corrosive substances and galvanic protection for local areas where the coating wears or chips away. When both the steel and the coating become exposed to the corrosive medium, the galvanic coating will preferentially corrode, while the steel remains protected.

Galvanic coatings are more complicated than the simple barrier coatings. As sacrificial anodes, the coatings must be designed and tested for each exposure environment, as reversals and ineffectiveness in galvanic behavior may take place from environment to environment. Additionally, some highly resistive exposure environments do not lend themselves well to galvanic action of any sort. ^[25]

Although quite a deal of research has been conducted on the use of galvanic coatings in concrete, conflicting results have been reported. ^[4, 13, 25] In some cases, galvanic coatings have been seen to perform well, while in others, little benefits

have been realized. The galvanic coatings therefore represent an enigmatic solution to the problem of steel corrosion in concrete.

Within the class of galvanic coatings, two options are emerging as feasible concrete protection systems. The first is traditional galvanizing, which involves coating steel with molten zinc. A coating system of pure zinc and zinc-rich alloys is produced in this approach. A second, more recent galvanic coating involves the use of zinc-rich paints. In this system, zinc is bound in an inorganic polymer matrix to the surface of the steel. This zinc-rich matrix forms the coating. The following chapter will investigate some of the theoretical considerations that pertain to the use of zinc in concrete. This discussion will form the framework for subsequent experimental analysis.

CHAPTER 3

THE USE OF ZINC FOR CORROSION CONTROL IN CONCRETE

3.1 Zinc Corrosion Properties

Without a doubt, zinc is the most common material used in metallic coatings for steel. Zinc has is used extensively, in part, due to its inherent corrosion resistance. Zinc remains passive in most environments of pH 6-13; a pH range which encompasses most environmental situations. In contrast, steel remains electrochemically active and subject to severe corrosion up to a pH of 11.5. Steel is therefore much more prone to corrosion than zinc in most situations.

It is important to note, however, that the high pH found in concrete (12-13.5) should favor steel more than zinc. In fact, under ideal conditions, steel should not corrode at all in concrete environments. This pattern has not been observed to be the case. Zinc is 2.5-5 times more resistant to chloride than steel, and in concrete environments where steel has been observed to corrode, zinc will often demonstrate better corrosion performance.^[27] It must be reiterated, though, that a concrete environment is not ideal for zinc, and zinc will corrode.

Corroding zinc is usually not as harmful to reinforced concrete as corroding steel. Zinc oxide, zinc hydroxide, and calcium hydrozincate are typical zinc corrosion products in alkaline concrete environments, and produce an approximate 50% expansion, in contrast to the 200% expansion developed by corroding steel.^[13] Zinc corrosion therefore produces lower expansive stresses and causes less cracking in the concrete.

An important exception to this rule occurs in high concentration chloride environments. In locations where abundant free chloride ions are available, zinc hydroxychloride II ($Zn_5[OH]_8Cl_2 \cdot H_2O$) has been observed to form. This compound produces an expansion on the order of 350%, creating much greater internal stresses than most iron oxides.^[13] A number of surprising corrosion failures in concrete of zinc-protected steel have been attributed to the formation of zinc hydroxychloride II.

The primary benefit of zinc, however, does not come from its inherent corrosion resistance. Many metals and alloys, such as nickel, tin, titanium, and platinum, are more corrosion resistant than zinc. It is the electrochemical relationship between zinc and steel that makes zinc unique among the corrosion resistant metals. Zinc will sacrificially protect steel when a galvanic couple is established. Zinc is the most economically feasible metal to offer such a galvanic relationship with steel.

The nature of the galvanic relationship between steel and zinc changes from environment to environment. It is therefore necessary to study this couple very specifically inside concrete in order to evaluate its corrosion protection effectiveness. One recent study has been conducted on zinc-coated steel in concrete, and a three-stage corrosion progression has been proposed.^[27] The stages are described below.

INITIATION: In the initiation stage, the zinc in the coating becomes passivated. The outer layers of zinc react with the alkaline concrete environment to produce protective oxides such as zinc oxide, zinc hydroxide, and calcium hydrozincate. These passivating reactions require a minimum amount of zinc to be present in the coating, consuming approximately 10 microns of pure zinc. Once

passivated, the zinc coating undergoes very little corrosion. Corrosion is therefore effectively prevented, unless the environment is disturbed in some way.

PROTECTION: The protection stage begins when the zinc passivation either breaks down or fails to develop. If not enough zinc is present in the coating, the initiation stage may be bypassed altogether, and the protection stage will take place first. Protection will otherwise begin if the chloride concentration reaches a threshold level (2 - 5 times the threshold for steel), the pore water pH drops below 6 or increases above 13.3, or breaks in the zinc coating promote galvanic action. During protection, the zinc dissolves unchecked. The rate of corrosion is usually lower than steel for the same chloride concentration. The protection stage continues until environmental changes allow the zinc to repassivate (initiation stage), or all the zinc becomes corroded.

PROPAGATION: The propagation stage takes over after all the zinc has been exhausted. The steel corrodes as if there were no protective zinc coating. Cracking and failure of the concrete will usually take place quickly after the start of propagation.

It is worth noting that 4-5 times longer is required for galvanized steel to reach the propagation stage than for uncoated steel to reach severe corrosion in identical exposure conditions. Therefore, definite benefits are possible with zinc corrosion protection in concrete.

3.2 Methods of Application

Galvanizing is the oldest method of applying zinc coatings to steel. In galvanizing, prepared pieces of steel are dipped in a molten bath of pure zinc at temperatures of approximately 450° C. The zinc metallurgically bonds to the surface of the steel, creating a multi-layer coating of pure zinc and zinc-rich alloys. Galvanized coatings adhere very well to the steel and are tough and abrasion resistant. A drawback of galvanized coatings is that they are expensive and are restricted to steel sizes and shapes that can be dipped in a zinc bath. Galvanizing is not practical with vary large or irregular pieces of steel.

Plating and electrogalvanizing are alternate methods for applying pure metallic zinc to steel surfaces using externally applied voltage. The cold plating processes result in thinner coatings, and are typically used either in conjunction with other coatings, or on parts that may be damaged by high temperatures. ^[20]

A final method of zinc application that has developed more recently is the use of zinc-rich paints. As mentioned previously, zinc paints bind particles of zinc to the steel in a polymer matrix. Zinc-rich paints may be heat-cured, post-cured, or self-curing. Below is a discussion of the historical development of inorganic zinc coatings. Particular attention will be given to a specific new class of zinc-rich paint: the inorganic, high-ratio zinc silicates.

3.3 Inorganic Zinc Coatings

3.3.1 Historical Development

Inorganic zinc coatings were first developed and used in Australia in the 1930's by Victor Nightingale, who mixed zinc dust in an alkaline sodium silicate solution, applied the mixed solution to a steel surface with a brush, and baked the coated steel in an oven.^[20] The baking process cured the coating, changing its mechanical and chemical properties. Variations of this heat-cured inorganic coating were used in Australia throughout the 1940's with remarkable success. Several applications performed satisfactorily for 50 years, greatly exceeding the original 20-year guarantee.

The baked coatings, however, were not practical for large applications such as ship hulls, storage tanks, and structural steel, due to size constraints. The next step was the development of an inorganic zinc coating that could be cold-cured through the application of a curing solution. In 1952, a successful post-cured coating was developed that used a zinc and sodium silicate organic base with a dibutyl amine phosphate curing solution. This coating represented a revolution in corrosion protection because it possessed good mechanical properties, it functioned well as corrosion protection, and the coating could be applied to steel of any shape and size.^[18]

While an improvement over the early heat-cured coatings, the post-cured coatings still required a two step application process, followed by a washing operation to remove the post-cure solution from the surface. A less time and material-intensive process was desired. The next logical step was to produce a self-curing coating that could be applied in one process. Several classes of self-curing inorganic zinc coatings have been developed and put into use.

One group of self-cure coatings is the alkali silicates. The alkali silicates are water-based, utilizing alkali inorganic zinc silicate. These coatings cure by water evaporation. Unfortunately, the alkali silicates cure slowly and tend to crack while drying.^[24] These coatings therefore represent a less than completely satisfactory solution to the self-cure problem.

More success was found with the ethyl silicates, which use ethyl silicate as a binder for the zinc particles. The ethyl silicate and zinc are applied with an organic solvent, as opposed to water in the case of the alkali silicates. The ethyl silicate coatings demonstrate better mechanical properties than the alkali silicates, with faster curing times and much less tendency to crack while curing. The organic solvents, however, pose environmental problems, especially in light of recent legislation limiting the use of volatile organic compounds (VOC's).^[19]

The most recent development in self-cure inorganic zinc coatings are the high-ratio zinc silicates, developed by NASA in the late 1970's for the protection of rocket launchers. This new class of coatings is water based, yet demonstrates the mechanical properties of the ethyl silicates. The high ratio zinc silicates therefore combine the strengths of both the alkali silicates and the ethyl silicates.

The high ratio zinc silicates have shown considerable promise in the years since their release in the early 1980's. They have performed well in a number of severe marine environment applications, and have provoked interest in the use of these coatings in other situations. In particular, the high ratio zinc silicates have been proposed as a corrosion protection system for reinforcing steel in concrete.

3.3.2 High Ratio Zinc Silicate Coatings

The high ratio zinc silicates function fundamentally in the same way as the older alkali and ethyl silicates. A silica/alkali metal compound is added to a liquid medium (in this case water), where chemical reactions produce a polymer of silicic acid. When particulate zinc is added to this mixture, the zinc reacts with exposed OH groups to form a new silicon-oxygen-zinc polymer. It is this polymer that binds the zinc and forms the coating as the water evaporates and the material cures. [20]

The high ratio zincs differ from earlier self-cure formulations, however, in that they use an improved silica/alkali binding compound. The high ratio silicates make use of a potassium silicate that has been post-processed and refined to increase the ratio of silica to potassium. The refined potassium silicates have a silica-to-potassium ratio of 5.3:1 (or higher), in contrast to the 3.2:1 ratio used in older formulations. [18] This higher silica content produces more reactive OH groups when the potassium silicate hydrolyzes with the water. As a result, the zinc reacts more rapidly, and the eventual coating possesses better corrosion and mechanical properties than the older self-cure coatings.

As barriers, the high ratio zinc silicates present somewhat of a technological breakthrough. The zinc silicate matrix becomes harder and more durable over time as a result of chemical reactions produced by normal exposure. Moisture and carbon dioxide in the air form carbonic acid within the coating. The carbonic acid ionizes the zinc particles, allowing the zinc to react further with the zinc silicate. This ongoing reaction makes the coating more dense and metal-like, and improves adhesion to the metal substrate. [20] In addition, the ionized zinc also forms zinc carbonate and zinc hydroxide in the pore spaces of the coating, sealing the coating

and reducing porosity. The high ratio zinc silicate coatings therefore tend to become more tough and durable in response to exposure, rather than deteriorate.

The zinc silicate matrix gives this class of coatings a distinct advantage over pure metallic coatings, such as galvanizing. The zinc silicate matrix is chemically inert and unreactive in most environments.^[20] Under severe exposure, the matrix slows down the corrosion of the zinc particles, giving the coating a longer life than pure metallic zinc.

Extensive atmospheric testing has been done on the high ratio zinc silicates in recent years. Below is a list of advantages found.^[24]

1. Rapid cure, with water resistance obtained in approximately 2 hours.
2. Excellent resistance to mudcracking during cure with coating thickness' in excess of 3 mils.
3. Exceptional hardness obtained in 2 hours.
4. Good adhesion to properly prepared steel surfaces.
5. Easy application with a variety of spray equipment.
6. Easy cleanup with water; environmentally friendly.
7. Exceptional atmospheric corrosion protection without topcoating.
8. Simple repair/recoating procedures.
9. Low maintenance requirements.
10. Lower cost than multi-coat organic coatings

A criticism of the high ratio zinc silicates is that the coatings cannot be applied in excess of 8 mil layers without problems occurring during cure. If the

outer layer of the coating is allowed to dry faster than the interior, drying stresses may produce a pattern of cracks known as mudcracking.^[24] It was also found that formation of an exterior crust may leave the underlying coating uncured and vulnerable to damage.

Curing conditions are also important. In cool, humid environments, the water in the coating evaporates more slowly and the coatings take longer to cure.

Finally, the coatings were found to take a significant time (4-6 months) to reach peak hardness and complete zinc saturation. Adequate hardness for handling may be obtained within hours, however.

Although these problems must be considered, they do not obscure the fact that the high ratio zinc silicates have performed very well in a number of applications, both in terms of corrosion protection and economics. The high ratio zinc silicate coatings therefore show considerable promise.

3.3.3 The Use of the High Ratio Zinc Silicates in Concrete

The high ratio zinc silicates have been proven very effective in atmospheric corrosion protection. However, much less testing has been done to date in concrete environments, and early testing did not yield promising results. Experiments conducted previously at the University of Texas at Austin^[12] found that when placed in concrete, the high ratio zinc silicates failed to provide galvanic protection for reinforcing steel.

It was postulated this failure resulted from bonding between the coating and the concrete. During autopsies, the coating was observed to bond to the concrete and pull away from the steel. If the concrete-coating bond did in fact interfere with the contact between the coating and the steel, this could very well have been the reason for the failures.

Other possible explanations include a lack of protective oxide formation in the zinc, and adverse pH effects. The first-generation of high ratio zinc silicates clearly did not perform adequately in a concrete environment.

A second-generation of high ratio zinc silicate has since been developed that does not bond to preferentially to concrete. This new coating is the subject of the current tests. It has been suggested that the different concrete-coating bond characteristics will result in improved corrosion performance.

3.4 Concluding Considerations: Zinc in Concrete

From the above discussion, it may be concluded that concrete is a complicated environment for zinc. Zinc has demonstrated widespread success in atmospheric exposure, but there are key differences between atmospheric and concrete exposure. In concrete, the pH is typically much higher than in the atmosphere, and zinc is sensitive to very high pH. In addition, there is much less oxygen present in concrete. This lack of oxygen at the anodes could prevent the formation of necessary protective zinc oxides within concrete, leading to possible rapid, and in some cases very expansive, corrosion of the zinc. Every proposed zinc-based protection system should therefore be tested fully within concrete before field implementation.

In spite of these causes for skepticism, some zinc coatings have shown considerable success where they have already been used in concrete. In a number of situations where both zinc-coated (galvanized) and uncoated reinforcing steel have been used in severe exposure, the zinc-coated bars have performed well, in marked contrast to the uncoated bars. One 21-year-old bridge in a marine environment

showed little or no corrosion of the galvanized reinforcing steel. In fact, it was estimated that 60-70% of the original coating still remained. ^[4]

Galvanizing remains an expensive option, though, costing approximately \$0.25 more per pound of steel than epoxy coatings. The high ratio zinc silicates, on the other hand, have proven to be very competitive in cost with other coating systems. ^[7]

When competitive pricing is combined with the fact that high ratio zinc silicate coatings are less sensitive to mechanical damage than non-galvanic systems, the zinc silicates should present an attractive option for concrete applications if testing proves them to be effective that environment.

CHAPTER 4

EXPERIMENTAL THEORY AND PROCEDURES

4.1 The Macrocell Method

4.1.1 Macrocell Theory

As mentioned, a macrocell is a corrosion cell where the anode and the cathode are separated; the anode steel is distinct from the cathode steel. Macrocell corrosion is forced corrosion resulting from a difference in potential between two areas of steel. Conductance between the two locations provides a link between the anode and cathode and allows corrosion to take place.

Microcell corrosion, in contrast, progresses with the anode and cathode in close proximity, often on the same piece of steel. The corroded area of steel will incorporate both the anode and apparently the cathode, at the same location. In reality, the anode and the cathode are separated, but the distance is very small. Pitting corrosion is an example of microcell action. In a pit, the tip of the pit forms the anode and the mouth of the pit acts as the cathode.

In this experiment, macrocells were constructed to study the corrosion behavior of a specific high ratio zinc silicate coating. The macrocells were fabricated by casting two layers of steel into blocks of concrete. The top layer of steel, or anode, was comprised of a single piece of reinforcing steel, bent into a "U" shape. The bottom layer of steel was placed 5 inches below the top steel, and was comprised of 3 straight pieces of reinforcing steel. Both layers of steel protruded from the front face of the concrete blocks. The bottom steel was connected electrically by welding a length of bar across the protruding ends.

To complete the macrocells, 4-sided acrylic dikes were fixed to the top of the macrocells with silicon adhesive, and a conductor of known resistance was used to connect the top and bottom mats of steel.

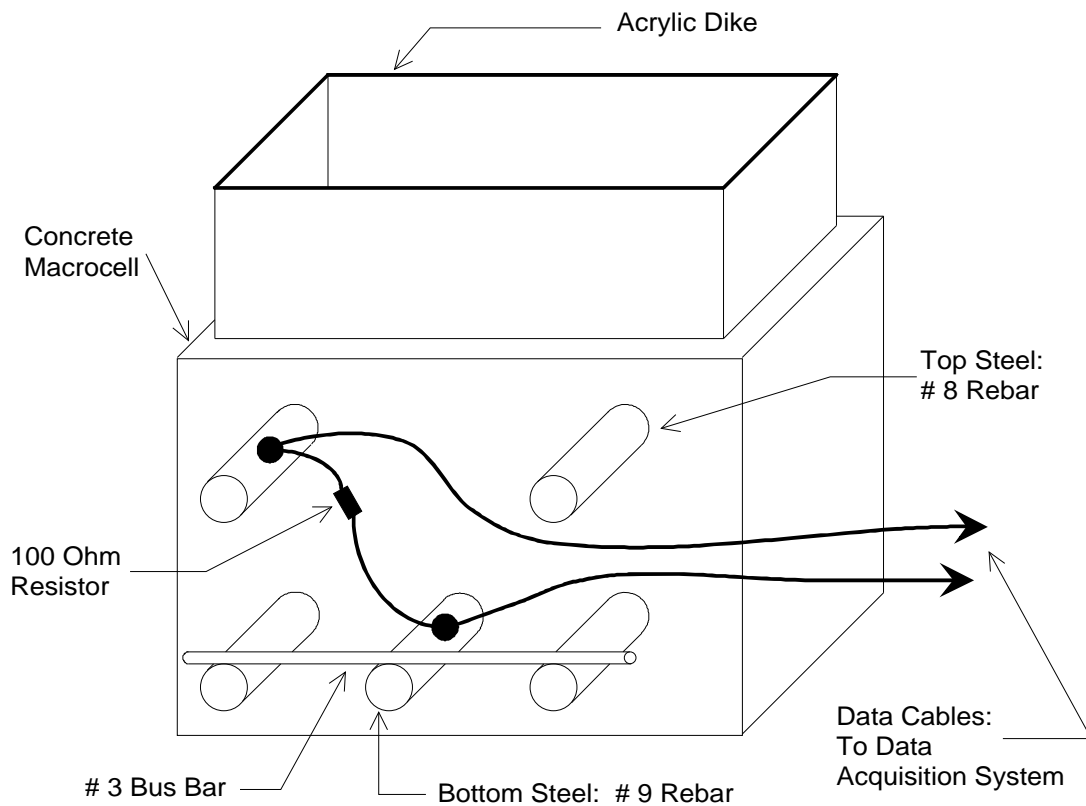


Figure 4.1: Key Macrocell Components

A data acquisition system was connected to the conductor, and was used to monitor the potential difference between the top and bottom mats of steel. Figure 4.1 illustrates the key components of the macrocells.

To promote corrosion, a 3.5 NaCl solution was ponded on top of the macrocells in 14-day wet, 14-day dry exposure cycles. The wet and dry cycles produced a more severe exposure condition than constant ponding due to the higher levels of oxygen maintained in the concrete. Evaporation of the salt solution was minimized by covering the dikes with pieces of 1/4" plywood.

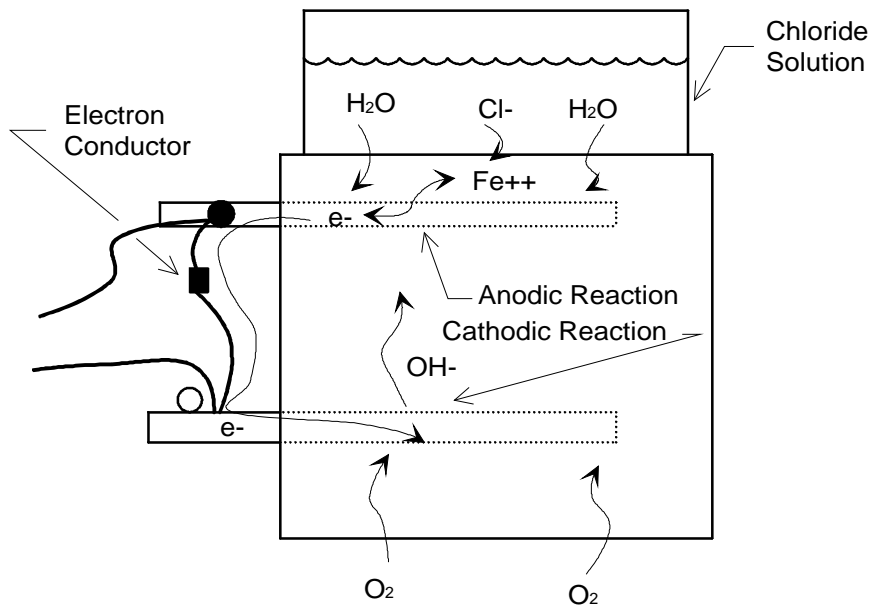


Figure 4.2: Macrocell Corrosion in Test Set-Up

During exposure, as the water and salt penetrated the concrete to the top steel, the potential of the top steel became altered and the anodic reactions took place. Metal ions dissolved, liberating electrons. The electrons traveled from the top steel, through the conductor, to the bottom layer of steel where the cathodic reactions took place and completed the macrocell. Figure 4.2 illustrates this corrosion process.

The data acquisition system was used to take instantaneous potential difference readings between the top and bottom mats of steel at weekly intervals. From the potential difference and the known resistance of the conductor, the instantaneous current readings were computed according to Eq. 1, below:

$$i = V/R \quad (1)$$

The current is the result of the electron flow between the top and bottom mats of steel and therefore is considered to represent a measure of the corrosion activity at a given time. The corrosion current values were integrated over time using the trapezoidal method to estimate the total charge flow over the life of the experiment. The total charge flow represented the total number of electrons to pass from the top to the bottom mat of steel, and made it possible to predict the total corrosion damage to the anode.

The process where macrocell corrosion is induced, potential differences are measured, and corrosion currents and damage levels are assessed is known as the macrocell method.

4.1.2 Macrocell Specifications

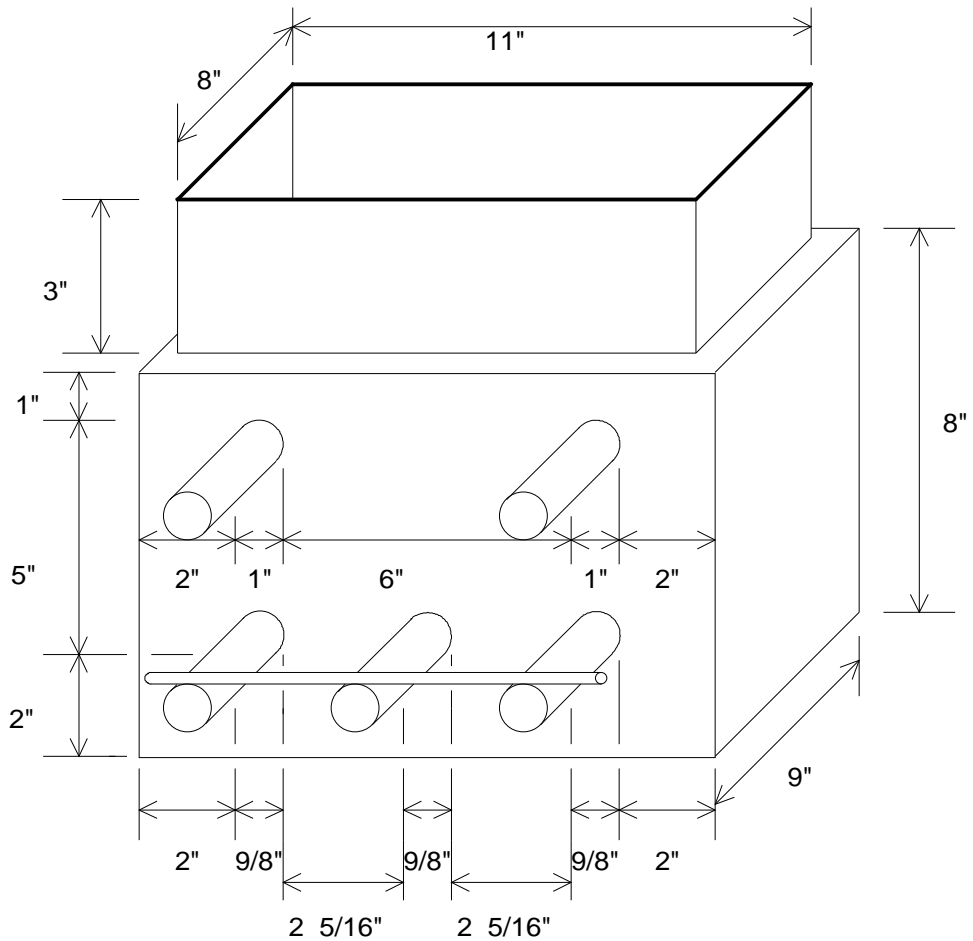


Figure 4.3: Macrocell Dimensions

The macrocell specifications were identical to the specifications used in previous research at The University of Texas investigating both epoxy bars and earlier high ratio zinc silicate coatings.^[12] Figure 4.3 gives an illustration of the macrocell dimensions and relative placement of the steel.

In previous research, both 1 in. and 2 in. cover over the top mat of steel were considered. The additional inch of cover was found to only delay, rather than prevent, the onset of corrosion.^[12] One inch of cover was used in all the macrocells in this study to minimize the time to corrosion.

As in the earlier zinc silicate research, a nominal 3000 psi concrete mix was selected. A low strength, high permeability mix was chosen to maximize the severity of chloride attack. The theoretical mix proportions are given below:

3/4" Aggregate:	1884 pcy
Sand	1435 pcy
Type II Cement	360 pcy
Water	266 pcy

Table 4.1: Theoretical Mix Proportions

Twenty-one 6"x12" standard cylinders were cast from the mix used in the macrocells. The cylinders were tested periodically for compressive strength. The strength gain curve is presented in Figure 4.4. It can be seen from the curve that the compressive strength corresponded very well with the 3000 psi design specification.

A chloride permeability test was conducted at approximately 90 days after casting. The test used was the "Rapid Determination of the Chloride Permeability of Concrete", AASHTO designation T 277-83. The concrete was found to pass 11,400 Coulombs of charge in 6 hours. High permeability concrete is defined as permitting over 4000 Coulombs of charge. The concrete therefore had a very high chloride permeability.

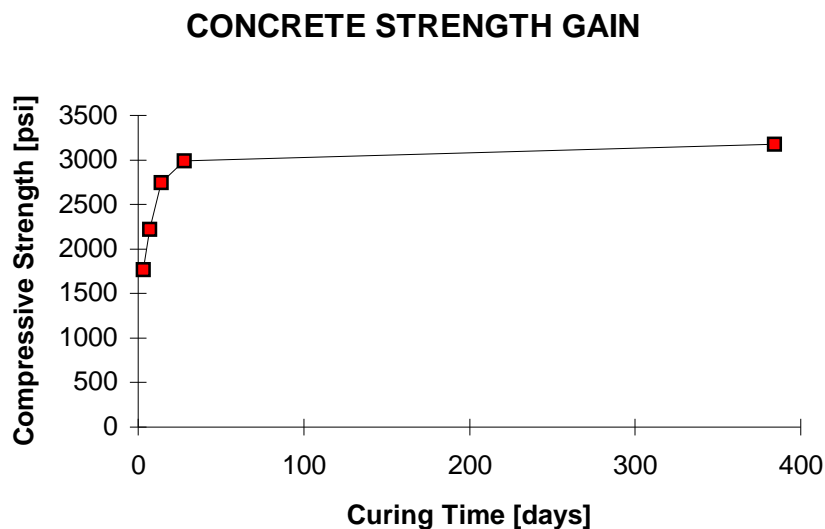


Figure 4.4: Strength Gain of Concrete Used in Macrocells

Fixed amounts of steel were used in the top and bottom mats. The anodes were all #8 bars bent in a "U" shape, with bend radii at least as severe as the guidelines specified in ACI 318-89. Out-to-out dimensions of the bent top bars varied between 6.25 in. and 8in. Different coating schemes were used on the top bars, according to the variables tested.

The bottom mats of steel were comprised of three, 12-inch lengths of straight #9 bars. The cathode steel was either coated with the inorganic zinc silicate, or left uncoated. As mentioned, the bottom steel was connected externally by welding a #3 bus bar across the protruding legs. All steel placed in the concrete was given at least 2 inches of cover on all sides except the protruding ends and over the tops of the anode bars. Short lengths of multi-stranded, insulated, copper wire were used to connect the top mats of steel with the bottom mats. One hundred-ohm resistors were inserted in the conductors between the top and bottom steel to

provide a measurable resistance to the corrosion currents. Sensors from the data acquisition system were installed at either ends of the conductors.

The dikes used to contain the chloride solution were constructed from 1/16" acrylic. The dimensions of the dikes were specified to allow them to fit within the footprint of the macrocells, standing 3 inches high. The dikes were fixed to the tops of the macrocells with silicon adhesive.

4.2 Experimental Variables

4.2.1 General Description of Tests

Nine groups of macrocells were constructed, with 3 cells in each group, yielding a total of 27 cells. Each group of cells was designed to investigate a specific set of coating variables. The different groups are described in section 4.2.2.

The macrocells were classified according to the coating scheme used on the anode and cathode steel. Six groups of cells contained anodes that had been coated with the second-generation high ratio zinc silicate. The anodes were coated, bent, and recoated, according to the desired condition, by the coating manufacturer. The zinc silicate coatings were either left unrepaired, were wire-brushed and repaired, or were grit-blasted and repaired. All zinc silicate-coated anodes were made from grade 40 steel, with the same deformation pattern and mill markings. The bars were used as supplied by the high ratio zinc silicate producer.

Two groups of cells used anodes that had been hot-dip galvanized. The galvanized bars were used as supplied by the zinc silicate coating producer. All galvanized bars were made from the same grade 60 steel. These bars were different,

both in terms of producing mill and steel strength, from the high ratio zinc silicate-coated anodes.

Finally, a single group of macrocells was constructed with epoxy-coated anodes. The epoxy coating was produced from NAP GARD 7-2709 powder, and was applied by a local epoxy coating supplier. The epoxy bars were all grade 60, were bent by the epoxy supplier, and were used "as received".

The bottom, cathode steel was either coated with the high ratio zinc silicate or left uncoated. In the case of the coated bottom steel, the bars were made from grade 60 steel and were used as supplied by the zinc silicate manufacturer. The uncoated cathode bars were made from same-heat, grade 60 steel obtained from a local mill.

Half of the macrocell groups used the black bar cathodes, while the other half used the coated cathodes. The epoxy specimens provided the only exception, using only coated steel for cathodes. It was felt that prior experiments had provided sufficient data on epoxy-coated samples with uncoated cathodes.

4.2.2 Description of Test Groups

As mentioned, 9 groups of macrocells were constructed, each with a different anode/cathode combination. The nine groups are described below.

Group 1: NB1-NB3: The NB group used anodes that had been coated with the high ratio zinc silicate coating, bent, and used "as received". No repair was done to the coating on the top bars. The NB group therefore tested a heavily damaged coating system. Uncoated cathodes were used.

Group 2: NC1-NC3: The NC group used anodes that had been bent and left unrepaired, identical to the top steel in group 1. Zinc silicate-coated bars were used for the bottom steel.

Group 3: WB1-WB3: The WB cells used top steel that was coated, bent, and repaired. The top bars were wire brushed to remove loose flakes of coating prior to repair. The WB group therefore tested one method of repairing the high ratio zinc silicate coating. The bottom bars were left uncoated.

Group 4: WC1-WC3: The top steel in the WC cells was identical to the top steel in the WB cells. The bottom steel was coated with the inorganic zinc coating.

Group 5: SB1-SB3: The SB group used top bars that were coated, bent, grit-blasted to remove loose flakes of coating, and repaired. The SB group therefore tested an alternate method of repairing the zinc silicate coating. Black bars were used for the bottom steel.

Group 6: SC1-SC3: The SC group, like the SB group, used top bars that were coated, bent, grit-blasted, and repaired. The bottom steel was comprised of the inorganic zinc coated bars.

Group 7: EC1-EC3: Macrocells in the EC group used epoxy-coated top steel supplied by a local epoxy coating manufacturer. The coating was made from a recent formulation NAP GARD 7-2709 powder. Zinc silicate-coated bars were used for the bottom steel.

Group 8: GB1-GB3: The GB group used top steel that was hot-dipped in zinc, bent, and used with no repair to the coating. The bars were used as supplied by the zinc silicate manufacturer. Uncoated cathode steel was used.

Group 9: GC1-GC3: The GC cells, like the GB cells, used top bars that were galvanized, bent, and used unrepaired. The bottom steel was coated with the high ratio zinc silicate coating.

4.3 Condition of Steel Prior to Concrete Placement

Prior to concrete placement, detailed observations were recorded for all steel bars for later comparison.

4.3.1 Unrepaired Zinc Silicate Coating (NB, NC)

The unrepaired, zinc silicate-coated anodes (Groups NB and NC) were the most heavily damaged of the zinc silicate bars. Figure 4.5 shows the condition of unrepaired bars prior to casting the concrete. As can be seen in Figure 4.5, extensive damage to the coating was present around the bend radius. Much of the original zinc silicate flaked off the steel as the bar was deformed in the 180 degree bend, leaving behind a gray residue where the coating once adhered. Patches of coating remained intact around bar deformations. Extensive areas of damage also were found away from the bend where the mandrel had contacted the outer edge of the bar. Mandrel damage extended in a line approximately 7 1/2 inches long, terminating at the start of the bend. Figure 4.6 shows the mandrel damage.

The unrepaired bars represented a severely distressed coating. Significant corrosion damage may be anticipated if the high ratio zinc silicate coatings do not offer some measure of galvanic protection to the steel.

Figure 4.5: Unrepaired High Ratio Zinc Silicate Coatings

Figure 4.6: Mandrel Damage to Unrepaired Zinc Silicate Coatings

4.3.2 Wire Brushed and Repaired Zinc Silicate Coatings

The WC and WB groups of macrocells used anodes that had been coated with the high ratio zinc silicate coating, bent in a 180 degree bend, and then wire brushed and repaired by spraying more zinc silicate on the damaged areas. The repaired coatings were in much better condition prior to concrete placement than the unrepaired coatings. Figure 4.7, below, gives an illustration of the wire brushed and repaired zinc silicate coatings.

Figure 4.7: Wire-Brushed and Repaired Zinc Silicate Coatings

Small amounts of damage were visible on the repaired coatings, as shown by Figure 4.7. Localized wearing of the coating, primarily on the bar deformations, had taken place during the shipping and handling of the bars. In the case of bar WB3, the mandrel damage had not been completely covered in the repair process. In addition, there was some localized mudcracking to the coating where the zinc

silicate had been applied too thickly. The repaired coatings, on the whole, were in very good condition, but they were not completely without damage.

4.3.3 Grit-Blasted and Repaired Zinc Silicate Coatings

Figure 4.8, below, gives an illustration of the SB and SC bar condition. Bars in the SB and SC groups were coated, bent, grit-blasted to remove any loose coating, and repaired.

Figure 4.8: Grit-Blasted and Repaired Zinc Silicate Coatings

The grit-blasted and repaired bars were very similar in quality to the wire brushed and repaired bars described in 4.3.2.

As with the wire brushed bars, the grit-blasted bars showed small localized areas of damage where either wearing had taken place or prior damage had not been completely repaired. Some mudcracking was visible.

4.3.4 Galvanized Bars

The galvanized bars were supplied by the high ratio zinc silicate manufacturer. In every case, the galvanized coating was in very poor condition. The bars had been galvanized prior to bending, and the bending process caused most of the metallic zinc to flake off the bars around the bends.

Figure 4.9: Condition of Galvanized Steel

Any zinc that remained on the bends was loosely attached to the bar deformations. Significant mandrel damage had also occurred on the outside of the bend. The areas of steel not covered by the galvanizing was dark brown and in the early stages of

corrosion. It was postulated that the steel had not been prepared adequately prior to galvanizing, resulting in a poor coating even before bending damage occurred. Figure 4.9 illustrates the condition of the galvanized coating in the region of the bends.

The unrepaired galvanized bars were included in the macrocells to provide a comparison to the unrepaired zinc silicate bars. However, the galvanized bars seemed to be in worse condition than the unrepaired zinc silicate bars. The galvanizing did not appear to have been applied with the same care of bar preparation as the zinc silicate coating, and corrosion was evident on the galvanized bars prior to concrete placement. The galvanizing was not felt to be representative of a state-of-the-art galvanized coating.

4.3.5 Epoxy Coated Bars

The epoxy bars were supplied by the epoxy-coated steel supplier and were in excellent condition. Great care had been taken during bending and shipping. There were no visible breaks in the coating except where the bars had been cut. In field situations, epoxy coatings will invariably suffer some damage. The coating condition used in these tests was therefore not indicative of field exposure for epoxy coatings. Figure 4.10 shows a photograph of one of the epoxy bars as it was received from the manufacturer.

**Figure 4.10: Condition of Epoxy Coatings
Prior to Concrete Placement**

4.3.6 Bottom Steel

The cathode steel was either uncoated or coated with the high ratio zinc silicate. the coated bars were supplied by the zinc silicate manufacturer and were in good condition. Like the repaired anode bars, the bottom bars had localized areas of damage where the coating had worn away during shipping and handling, but in general, the coating was in very good repair. Figure 4.11 shows a coated bottom bar.

Figure 4.11: Condition of Zinc Silicate-Coated Bottom Steel

Figure 4.12: Condition of Uncoated Cathode Bars

The uncoated bottom bars were cleaned and prepared thoroughly. The bars were wire-brushed to remove all mill scale and then pickled in sulfuric acid several days prior to concrete placement to obtain a uniform electrochemical surface. Figure 4.12 shows an example of a black cathode bar.

4.4 Chloride Specimens and Tests

In addition to the 27 macrocells, 30 7"x7"x6" concrete blocks were cast. Like the macrocells, these blocks were fitted with acrylic dikes and were subjected to the same chloride solution exposure. The chloride cells were used to monitor the progression of chloride ions into the concrete.

At the end of every 28-day exposure cycle, one of the blocks was removed from the experiment and drilled to a depth of three inches. Samples of concrete powder were retained from the holes at quarter-inch intervals. This powder was then analyzed using a Rapid Chloride Test ^[22] to determine the percent concentration of chloride by weight of concrete. Chloride concentration depth profiles were then plotted for every month of exposure.

Chloride tests were also conducted during the macrocell autopsies. Dust was taken from each of the macrocells investigated at a depth of 1-2 inches immediately prior to both autopsies. At that time, dust was also taken from one of the chloride samples at the same depth range. The chloride concentration estimated by the chloride cell was then compared to the chloride concentration found in the macrocell. This comparison provided a means of assessing the consistency of chloride diffusion in concrete.

In past experiments, significant variability was found in the chloride concentration data. Two macrocells sampled from the same depths at the same time have yielded very different chloride concentration readings.^[12] This variability has been attributed to the lack of homogeneity in the concrete.

4.5 Construction of Formwork and Steel Placement

The forms for the macrocells and the chloride cells were constructed from 3/4" form-release plywood. For the macrocells, a single piece of plywood formed the base for a group of cells. Transverse lengths of plywood were fixed to vertical 2"x4" legs, which were in turn fixed to both the base plate and to 2"x4" wales around the base perimeter. Smaller longitudinal pieces of plywood separated the backs of the cells. The macrocell face plates were drilled to accommodate the top and bottom steel, and were screwed in place to the vertical legs after the top steel had been added. Longitudinal wales were also fitted to the outside faces of the macrocells at the level of the top steel. The top wales were used to hold the anode steel in position. Finally, transverse bracing was added to the tops of the vertical legs to increase the rigidity of the formwork. Figure 4.13 shows the formwork upon completion.

Figure 4.13: Completed Macrocell Formwork

The final step in formwork construction was to secure the steel in place against movement. Once positioned, the top steel was anchored with wire ties wrapped around the protruding ends. The bottom steel was held in place by driving

wedges under the ends of the bars. Figure 4.14, below, shows the top and bottom steel anchored in position prior to concrete placement.

Figure 4.14: Top and Bottom Steel Anchored in Place

The chloride cell formwork was constructed similarly to the macrocell formwork. However, due to the smaller size of the chloride cells, the transverse bracing, legs, and top wales were omitted. Figure 4.15 shows the completed chloride cell formwork.

Figure 4.15: Completed Chloride Cell Formwork

4.6 Concrete Placement

The concrete was placed in one lift using a wheel barrow and shovel. A vibrator was used to consolidate the concrete in each cell. In the macrocells, the vibrator was applied carefully at the back of the cells to avoid shifting the steel or damaging the coatings.

Twenty-one 6"x12" cylinders and four 4"x8" cylinders were cast from the same mix. Standard lifts and consolidation procedures were used in placing the cylinders. The cylinders were later used for strength and permeability tests.

After placement, all cells and cylinders were screeded, trowelled, and hand-finished. The concrete was then covered with plastic and allowed to cure on

location. The formwork was stripped approximately 2 weeks after placement. All cylinders, macrocells, and chloride cells were removed from the forms at the same time.

4.7 Sample Preparation

The final modifications were made to the macrocells in a two-week period following removal from formwork. First, short lengths of #3 reinforcing steel were welded across the ends of the cathode bars in each cell. These bus bars provided an electrical connection between the three #9 bars in the bottom mat of steel.

Two coats of water sealer were then applied to the side faces of the macrocells and chloride cells. The water sealer was designed to both prevent water leakage from the cells and to simulate an infinite slab with uniform lateral moisture content.

The free ends of the cathode bars were coated with a protective oil to prevent corrosion external to the concrete.

Next, acrylic dikes were attached to the tops of the macrocells and chloride cells. Silicon caulk was used because it adhered well to the concrete and provided a water-tight seal around the base of the dikes.

The last step in preparation was to assemble the conductor and data leads. Equal lengths of double-conductor digital cable were measured and cut for each macrocell. At one end, the digital cable was soldered to the conductor and resistor linking the top and bottom steel. The other end of the digital cable was connected to the computer interface for the data acquisition system. Electrical clamps were

placed on the top and bottom bars of each macrocell, and the conductors were attached with

Figure 4.16: Macrocells Prior to First Round of Tests

spade connectors to the clamps. Finally, the macrocells and chloride cells were arranged on a series of shelves and testing was begun. Figure 4.16 shows the macrocells in the test set-up prior to the first cycle of testing.

4.8 Evaluation of Macrocells

Three methods were used to evaluate the corrosion behavior of the coatings. First, the corrosion potential data were used to construct the corrosion current time histories and charge flow plots. These plots indicated the theoretical corrosion damage to the coatings. Higher currents indicated greater corrosion activity, and higher charge flow indicated greater cumulative corrosion damage.

Second, external observations were taken of the macrocells throughout the life of the experiment. Cracks and corrosion products were noted and described as they became evident on the exterior of the cells.

Finally, cells were removed from testing on two occasions and visual inspections were conducted. The first round of autopsies took place after seven months of exposure, when one third of the cells were taken out of testing. In each cell group, the median sample as defined by the predicted corrosion damage was selected for the autopsy. This selection process kept the cells with the highest and lowest levels of damage in the experiment.

To conduct the visual inspection, the selected cells were removed from the test apparatus and cut with a hand-operated circular concrete saw. Cuts were made around the perimeter of the macrocells at a level 1/4" below the bottom of the top steel. A single cut was made on the top face to a depth of 3/4", terminating 1/4" above the top face of the anode steel. Figure 4.17 shows the saw cuts that were made to the macrocells.

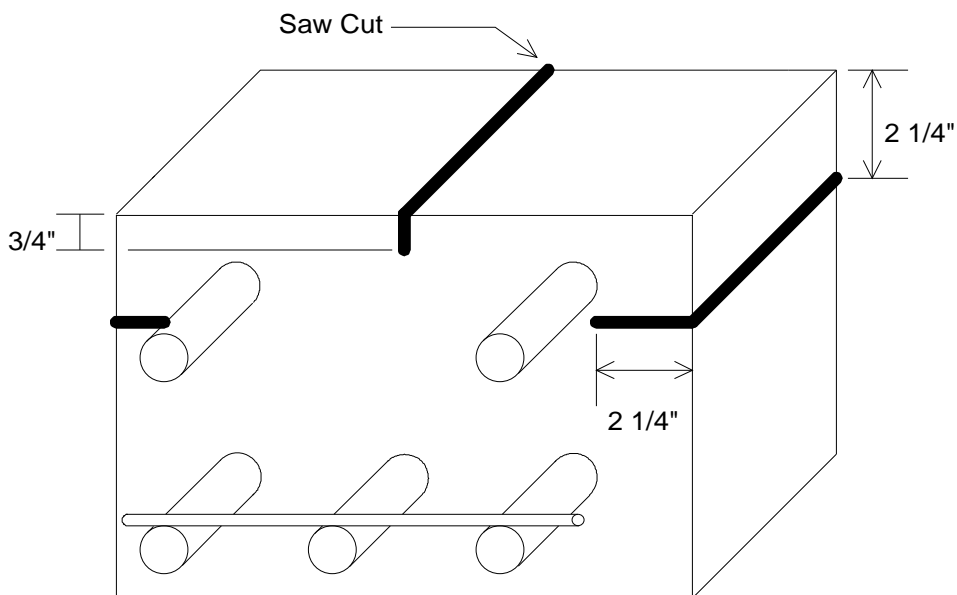


Figure 4.17: Diagram of Cuts Made to Macrocells

A pry-bar was inserted into the saw cuts and struck with a hammer, separating the top layer of concrete and anode steel from the rest of the macrocell. The legs of the top steel were then tapped with the hammer to remove any remaining fragments of concrete.

Each anode bar was examined carefully upon removal from the macrocells. Observations concerning the levels and locations of corrosion, and the corrosion products seen, were recorded. Photographs were also taken of each bar. All observations had to be taken quickly, as the corrosion products tended to react with the atmosphere and change color.

A second round visual inspections was conducted after thirteen months of exposure. The macrocells from each group with the highest corrosion currents and charge flux were inspected at that time. Observations taken in the second autopsy provided the last visual data to be included in this write-up.

4.9 Procedural Modifications

After 8 months of exposure, the front face of 1/2 of the remaining macrocells were coated with an epoxy patching compound. The cells with the highest corrosion current activity in each pair were selected for this treatment. The following were coated: NC3, NB3, WC2, WB2, EC3, SB3, SC1, GB1, GC2. In all cases except NC3, the cells chosen also had the highest cumulative charge flow in each pair.

This modification was performed to more effectively seal the macrocells from oxygen diffusion around the protruding bars. It was found in the first autopsy that corrosion on the zinc silicate-coated bars was concentrated in the first inch within the concrete. It was believed that the corrosion concentrated near the exterior face due to higher concentrations of oxygen. Oxygen participates in the cathodic reaction and in secondary reactions that consume dissolved metal ions.

The additional sealing was deemed acceptable because rarely in the field will reinforcing steel protrude from the concrete mass and become exposed to high levels of oxygen.

A second coat of epoxy sealer was applied to the same macrocells after 11 months of exposure. At that time, silicon caulk was also applied to the face of the cells around the anode bar legs to increase the effectiveness of the vapor barrier.

CHAPTER 5

TEST RESULTS

5.1 Introduction

The first exposure began on September 1, 1993, and continued for thirteen, 28-day exposure. Data from the nine test groups were taken at weekly intervals during this period. One specimen from each group was removed from testing after 7 and 13 months, and the bars were removed from the concrete for visual inspection. The corrosion current and cumulative charge flow data are presented and discussed, as well as the results from the two visual inspections. Finally, corrosion products and chloride concentration data are discussed in the final sections of the chapter.

5.2 Corrosion Current Data

5.2.1 Plots

Figures 5.1 -5.9 are presented below, and give the corrosion currents as a function of time for all the macrocell groups. The currents represent the flow of electrons from the top steel to the bottom steel. A high negative current is indicative of significant corrosion.

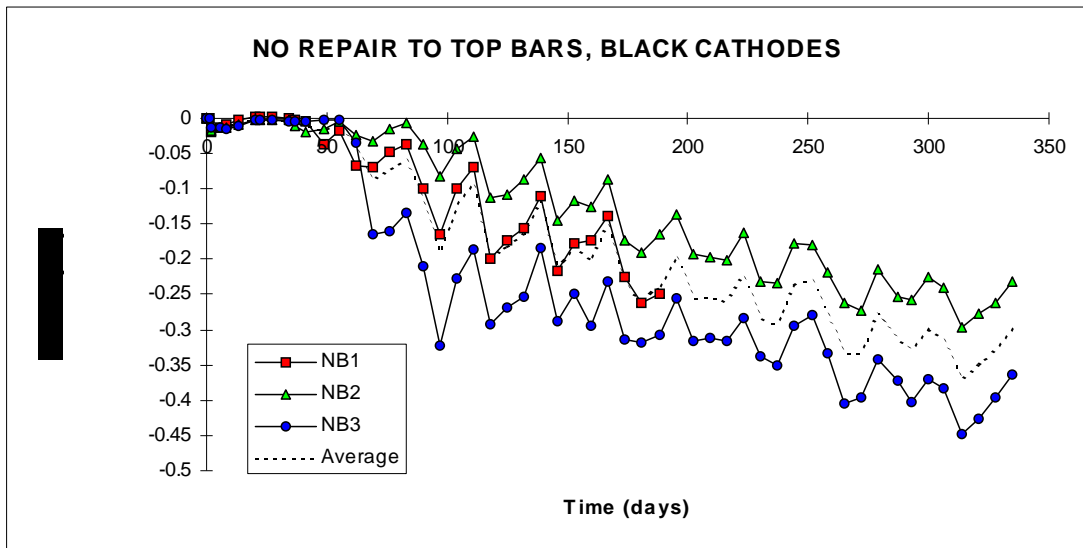


Figure 5.1: Corrosion Currents: Group 1

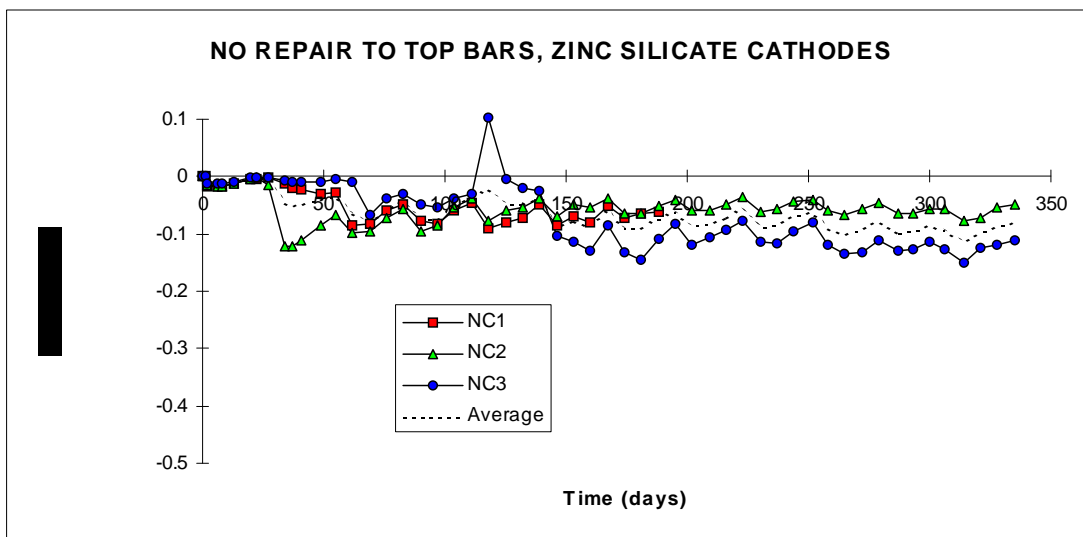


Figure 5.2: Corrosion Currents: Group 2

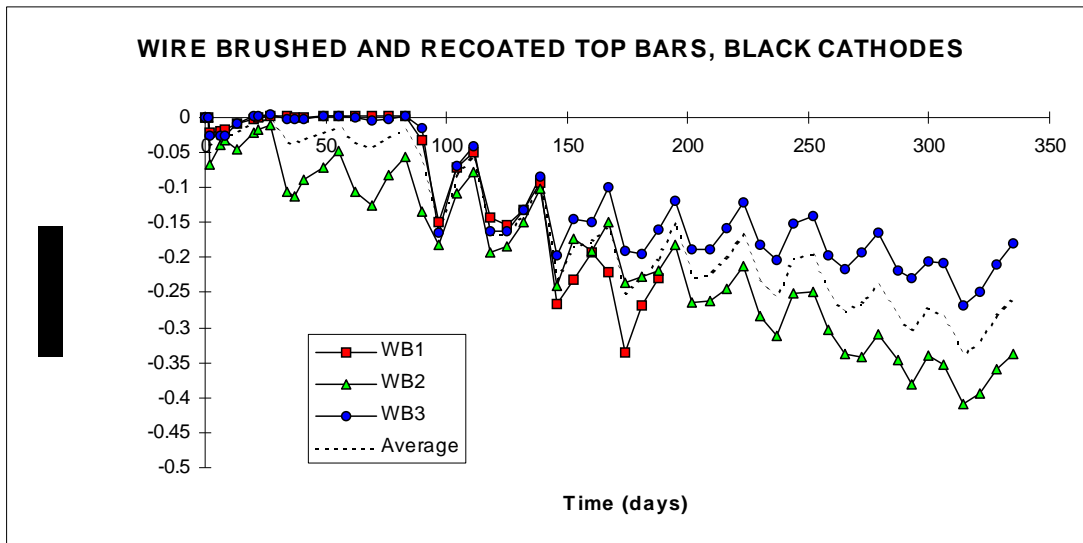


Figure 5.3: Corrosion Currents: Group 3

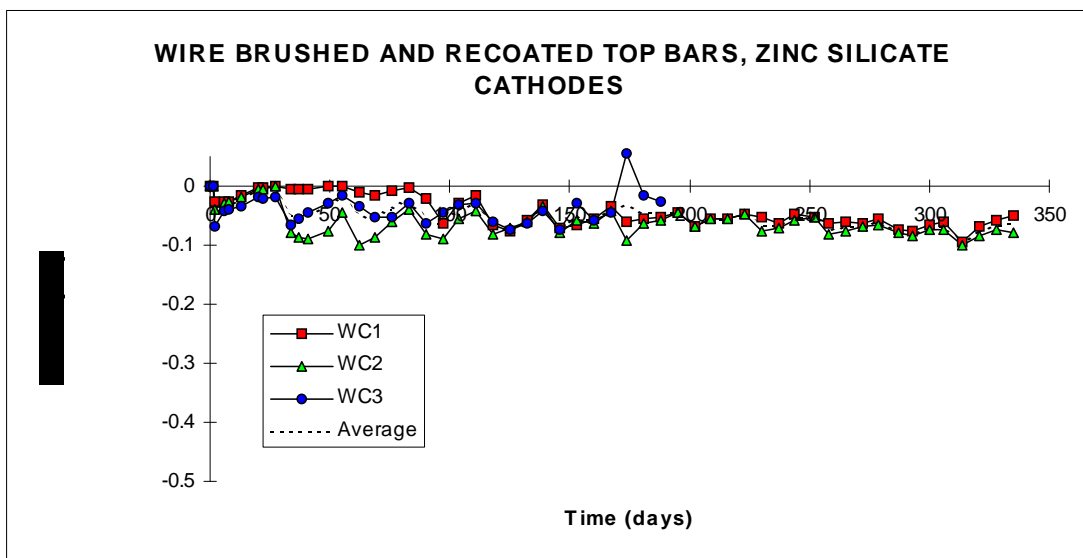


Figure 5.4: Corrosion Currents: Group 4

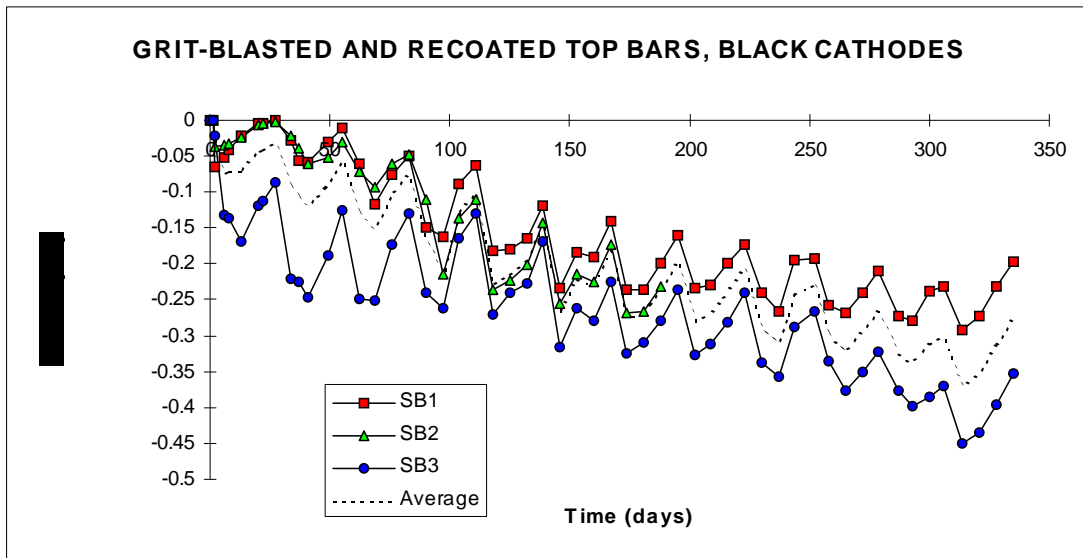


Figure 5.5: Corrosion Currents: Group 5

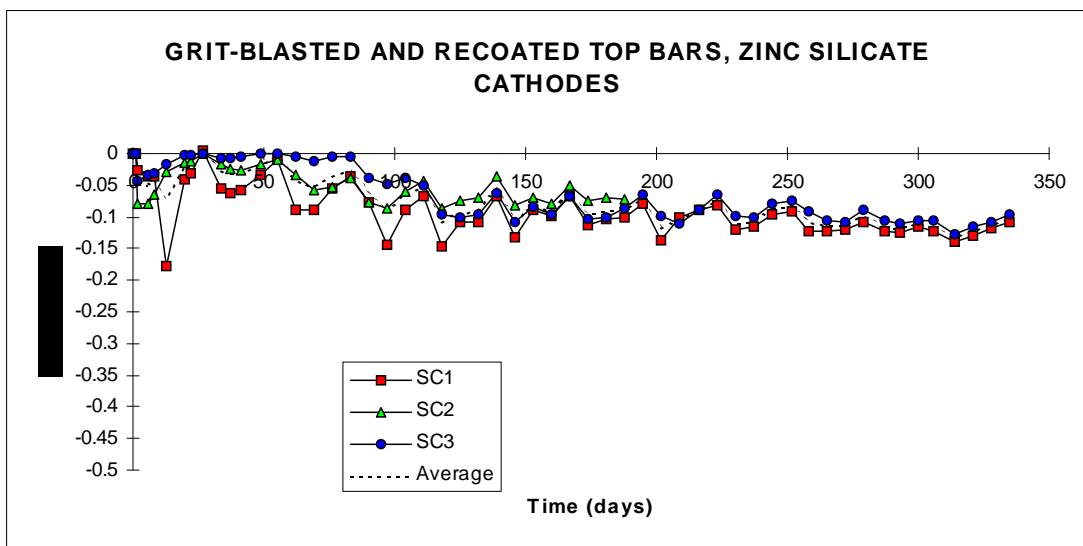


Figure 5.6: Corrosion Currents: Group 6

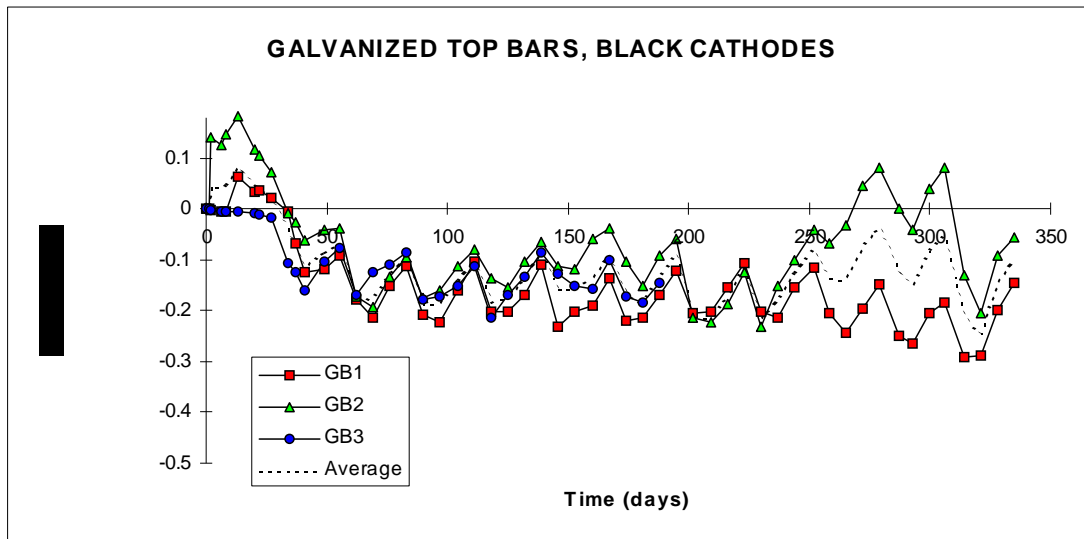


Figure 5.7: Corrosion Currents: Group 7

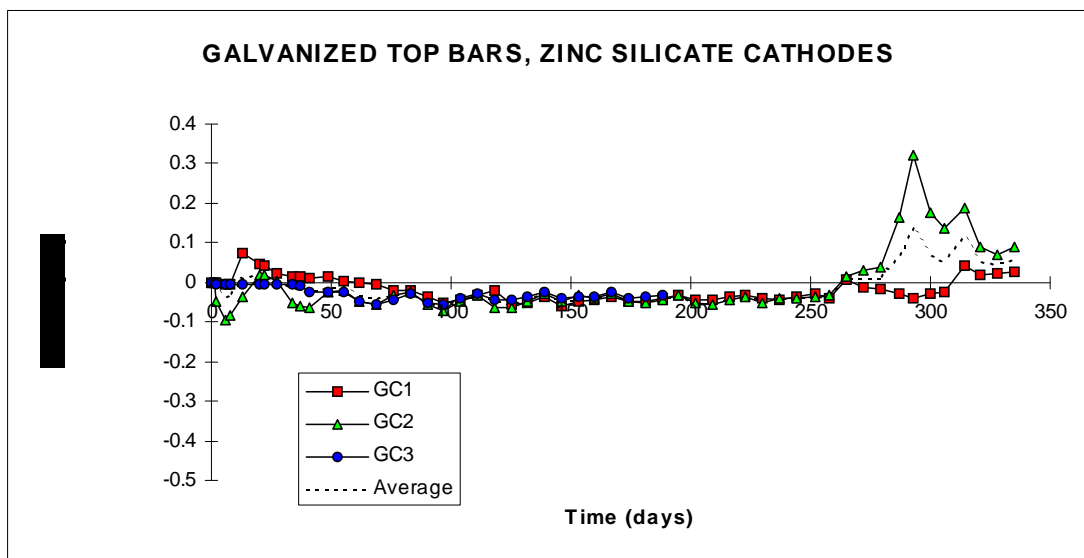


Figure 5.8: Corrosion Currents: Group 8

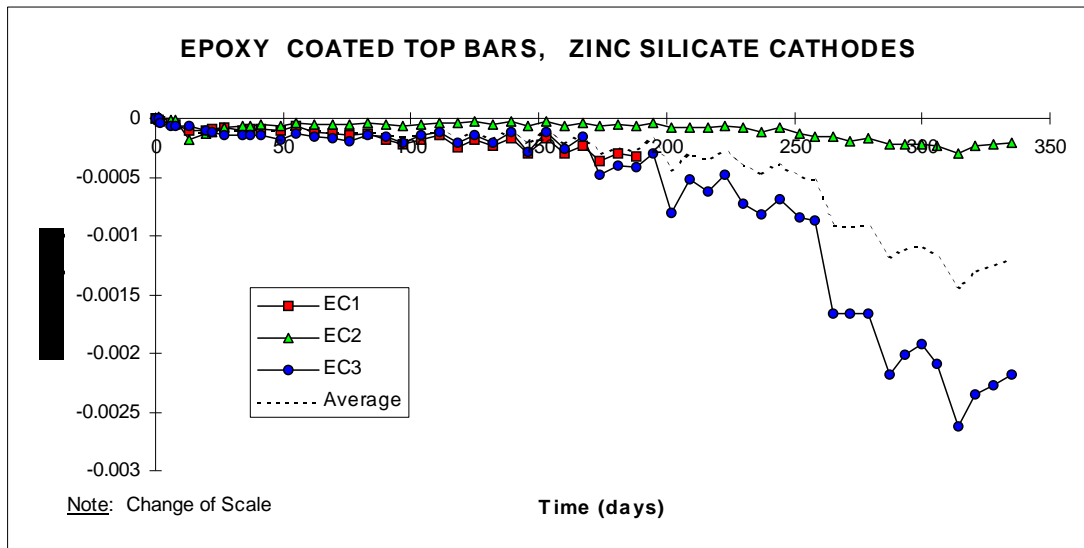


Figure 5.9: Group 9 Corrosion Currents

5.2.2 Analysis of Corrosion Current Data

High Ratio Zinc Silicate-Coated Top Steel: Analysis of the corrosion currents shows the approximate time when corrosion began to take place. In the case of the high ratio zinc silicate and galvanized top steel, the time to corrosion was approximately 50-90 days. The time to corrosion is indicated in each case by the first significant dip in the graphs.

Both the galvanized and the high ratio zinc coatings are active, in that the coatings themselves are expected to corrode when environmental conditions become sufficiently aggressive. The 50-90 day initiation time therefore indicates the time required for sufficient water and chlorides to diffuse through the one inch of concrete cover, underscoring the benefits of providing more cover.

The corrosion plots clearly delineate the exposure cycles. Once corrosion initiated, the beginning of the wet cycles became marked by a sharp decline in the corrosion current graphs. Almost all of the graphs show such peaks at 111 days,

corresponding to the start of the fifth exposure cycle. Subsequent peaks are spaced at 4-week intervals.

Figures 5.1-5.6 reveal several noteworthy differences between the high ratio zinc silicate specimens with uncoated and coated cathodes. The specimens with the coated bottom steel showed currents that were significantly lower in magnitude than the uncoated specimens. The coated macrocells, Figures 5.2, 5.4 and 5.6, showed maximum corrosion currents of -0.15, -0.10, -0.14 mA, respectively. The difference between peak and trough readings were approximately 0.05 mA, producing comparatively smooth corrosion current curves. Also, once corrosion became well established after 150 days of exposure, the long term increases in corrosion current magnitudes were very small. The corrosion rates did not appear to increase as the cycles continued.

In contrast, the macrocells with uncoated cathode steel demonstrated much greater corrosion activity. Figures 5.1, 5.3, and 5.5 show maximum corrosion current magnitudes of -0.45, -0.41, and -0.45, respectively. Typical differences between peak and trough current readings were approximately 0.2-0.25 mA, in contrast with the 0.05 mA differences seen with the coated-cathode samples. In addition, as the cycles continued past 150 days, the maximum corrosion current magnitudes steadily increased, indicating accelerated corrosion.

The difference in corrosion performance may be explained in terms of the anode/cathode ratio. In a corrosion cell, the cathode functions only as the site of an electron-consuming reaction. The coated bottom steel in the macrocells provided a more resistive surface than the uncoated steel, effectively shrinking the size of the available cathode. With smaller cathodes, identical anodes and equivalent exposure conditions, the samples with coated bottom steel had a much larger anode/cathode ratio than the uncoated samples. Less corrosion damage would be expected in the cells with the coated bottom bars, due to this higher anode/cathode ratio.

Finally with respect to the zinc silicate samples, very few differences may be seen between the three coating conditions. The unrepaired, wire-brushed and repaired, and grit-blasted and repaired showed very similar corrosion current patterns.

Epoxy-Coated Top Steel: The epoxy-coated samples showed a much longer time to corrosion than the zinc-based coatings, requiring a minimum of 200 days for corrosion to initiate (see Figure 5.7). The longer delay resulted from the inactive nature of the epoxy coatings. The time to corrosion was the time required for water and chlorides to both diffuse to the level of the top steel and penetrate the epoxy barrier. No barrier penetration was necessary to produce corrosion currents in the case of the zinc-based coatings.

The epoxy-coated samples showed much lower corrosion currents than all of the other coating schemes. The maximum corrosion current was -0.0026 mA. (Note that the scale used in Figure 5.9 is 1/100 of the scale used in all other figures.) This current was produced solely by the corrosion of the steel; there was no sacrificial metal in the epoxy coating to provide alternate currents.

Corrosion of epoxy-coated steel has only been known to occur where breaks occur in the coating, and the coatings used in these macrocells showed no visible damage prior to concrete placement. Therefore, the lower currents were expected.

Galvanized Top Steel: Overall, the galvanized samples demonstrated similar corrosion current behavior to the high ratio zinc silicate samples. The cells with uncoated bottom steel showed more activity than the samples with the coated bottom steel.

However, the corrosion current magnitudes were significantly lower with the galvanized samples than with the zinc silicate cells. The galvanized cells had a maximum corrosion current of -0.29 mA, compared to a -0.45 mA current with the zinc silicate specimens. Also, the galvanized-bar corrosion currents did not appear to increase with time on the same scale as the zinc silicate specimens. Less corrosion appeared to take place in the galvanized macrocells.

An anomaly did occur with the galvanized-bar specimens after approximately 250 days of exposure. In both the GB and the GC macrocells, the currents increased significantly in the positive direction. In the case of GC2, a maximum corrosion current of $+0.32$ mA was recorded at 293 days. The top steel in 3 of the remaining 4 cells similarly became cathodic to the bottom steel at about that time. This behavior corresponded approximately with the appearance of corrosion products and cracking on the top surface of the macrocells.

When the bars were inspected, it was discovered that some corrosion was taking place on the bottom steel within the concrete. It would therefore seem that as the zinc in the galvanized coatings became depleted, the top steel was not able to protect the bottom steel from corrosion as chlorides began to reach the level of the cathodes. Anodic dissolution then began to take place on both the top and bottom steel, disturbing the corrosion potentials.

5.3 Charge Flow Data

5.3.1 Plots

Figures 5.10 -5.18 are presented below, and give the plots of total charge flow as a function of time for all the macrocells. Values were computed by integrating the current vs. time graphs in section 5.2.1, using a trapezoidal approximation. The total charge flow indicates the number of electrons that have participated in macrocell corrosion. High negative values therefore indicate high predicted corrosion damage.

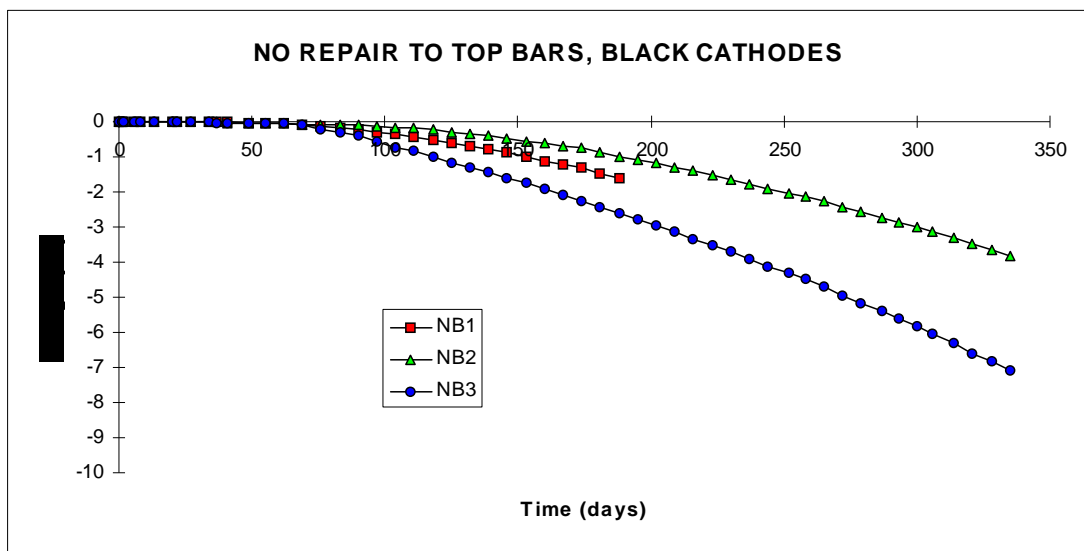


Figure 5.10: Cumulative Charge Flow/Damage: Group 1

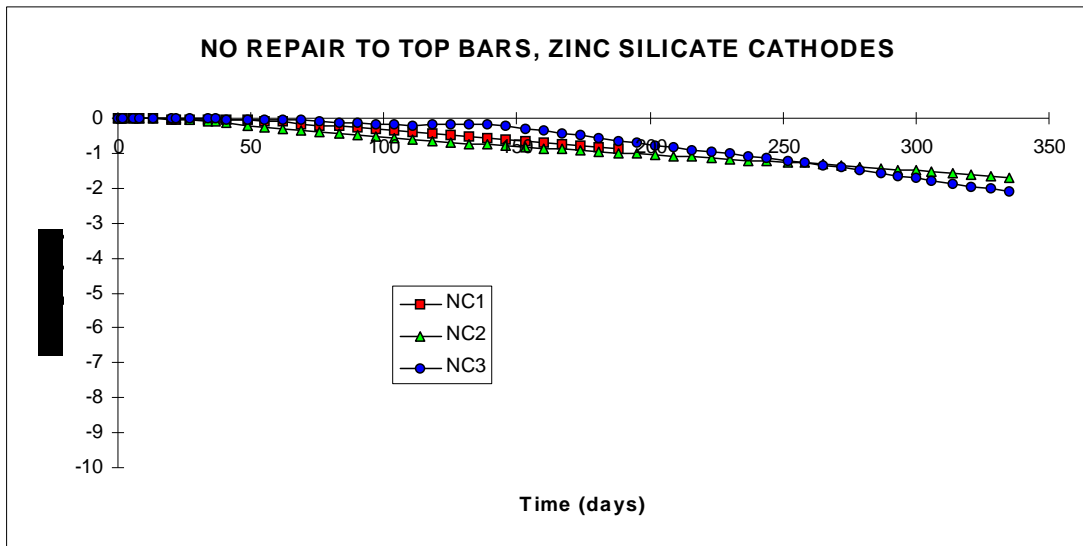


Figure 5.11: Cumulative Charge Flow/Damage: Group 2

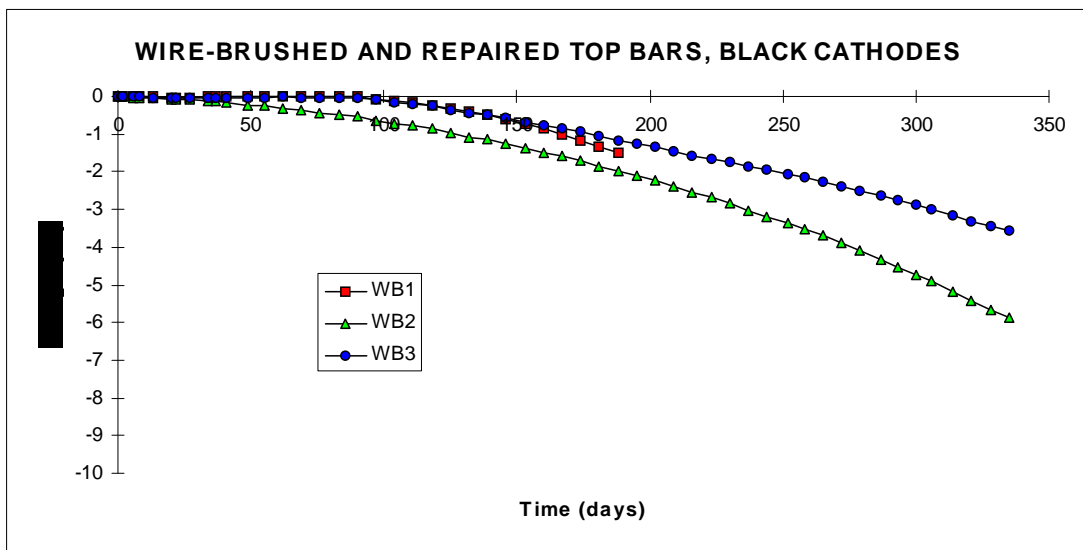


Figure 5.12: Cumulative Charge Flow/Damage: Group 3

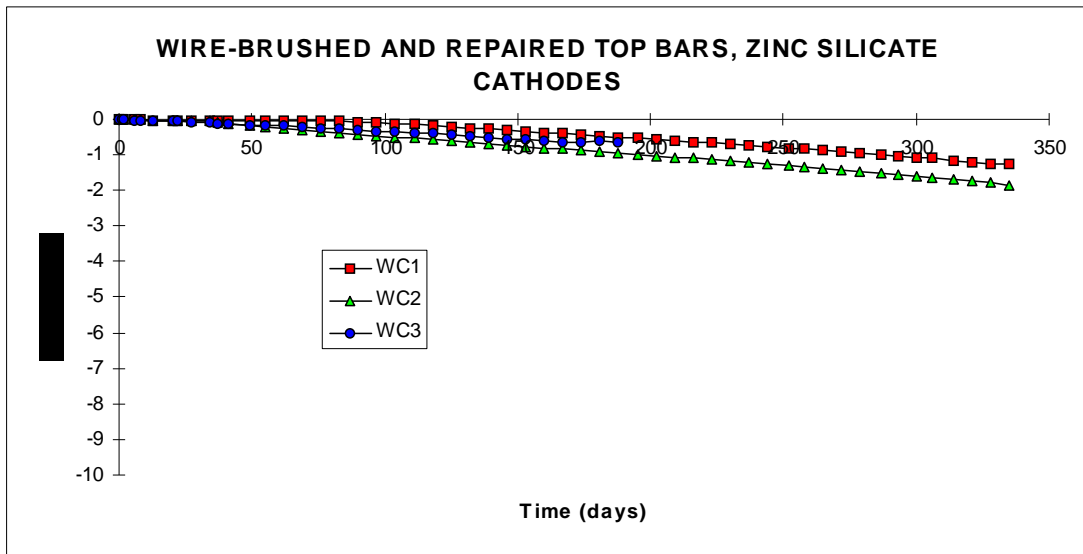


Figure 5.13: Cumulative Charge Flow/Damage: Group 4

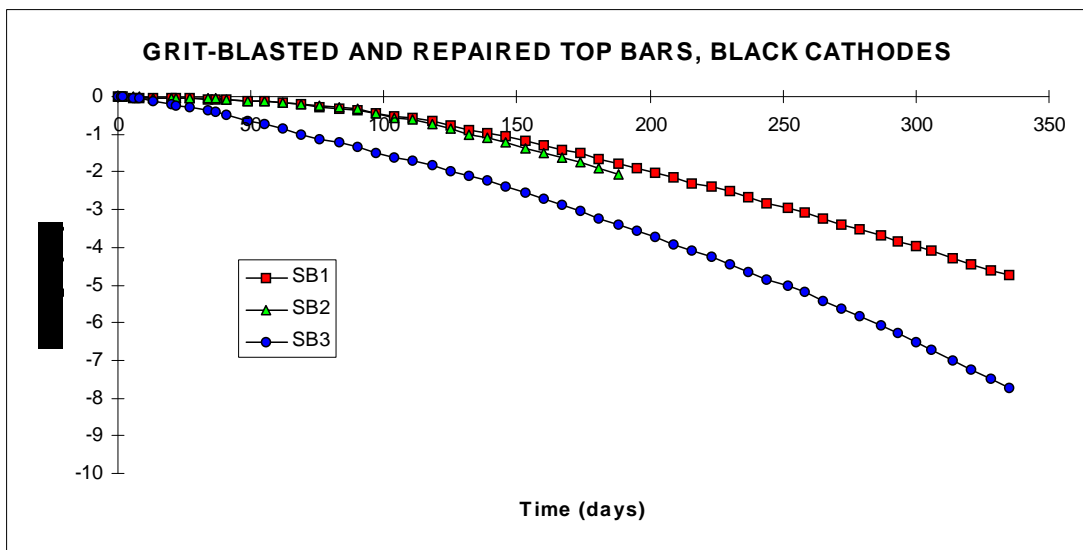


Figure 5.14: Cumulative Charge Flow/Damage: Group 5

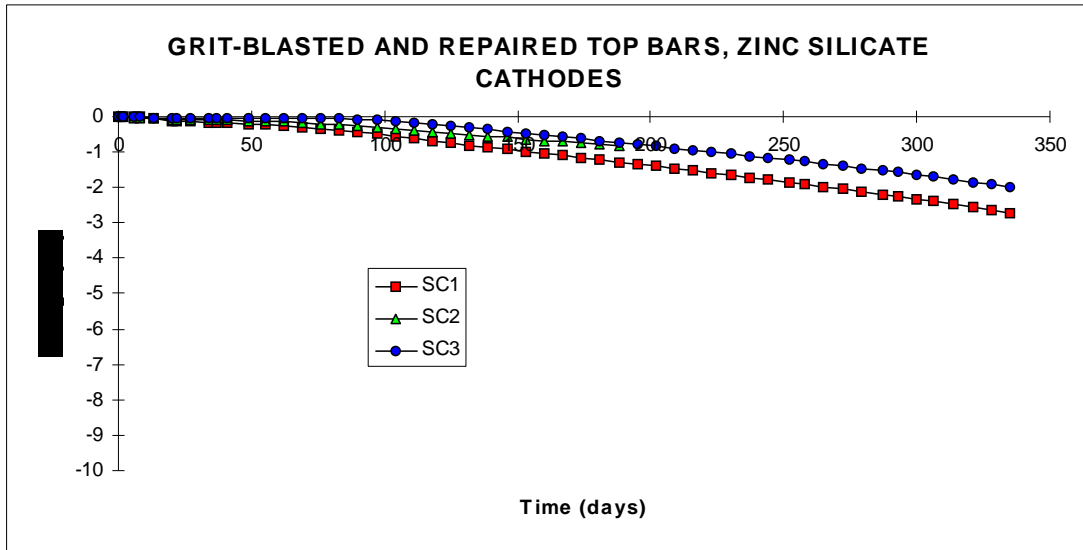


Figure 5.15: Cumulative Charge Flow/Damage: Group 6

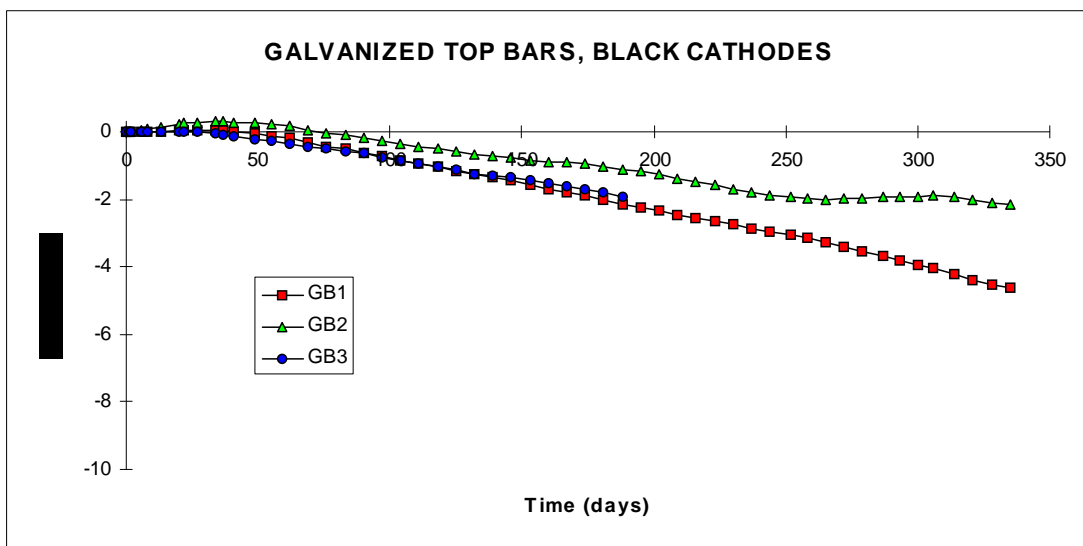


Figure 5.16: Cumulative Charge Flow/Damage: Group 7

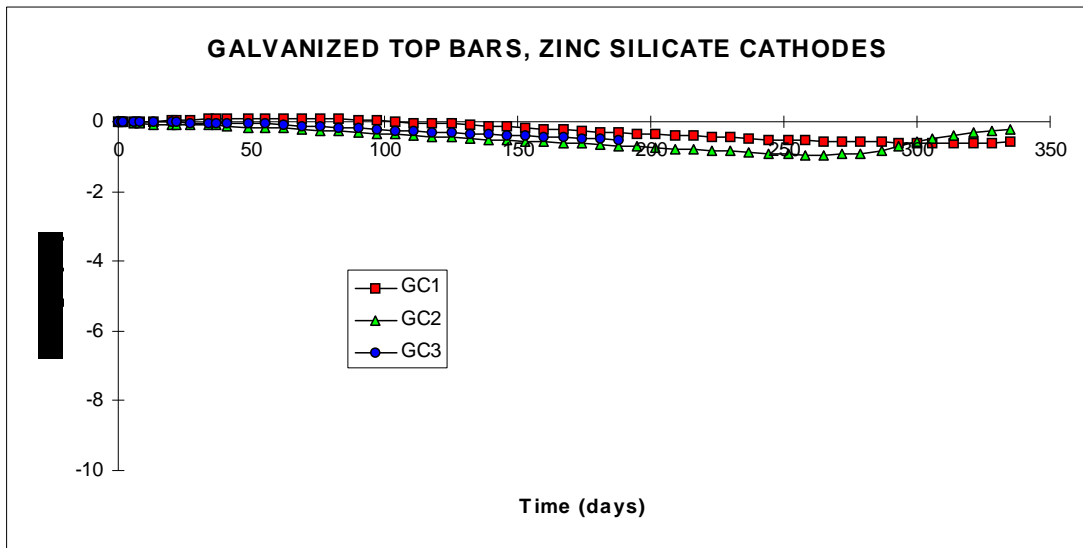


Figure 5.17: Cumulative Charge Flow/Damage: Group 8

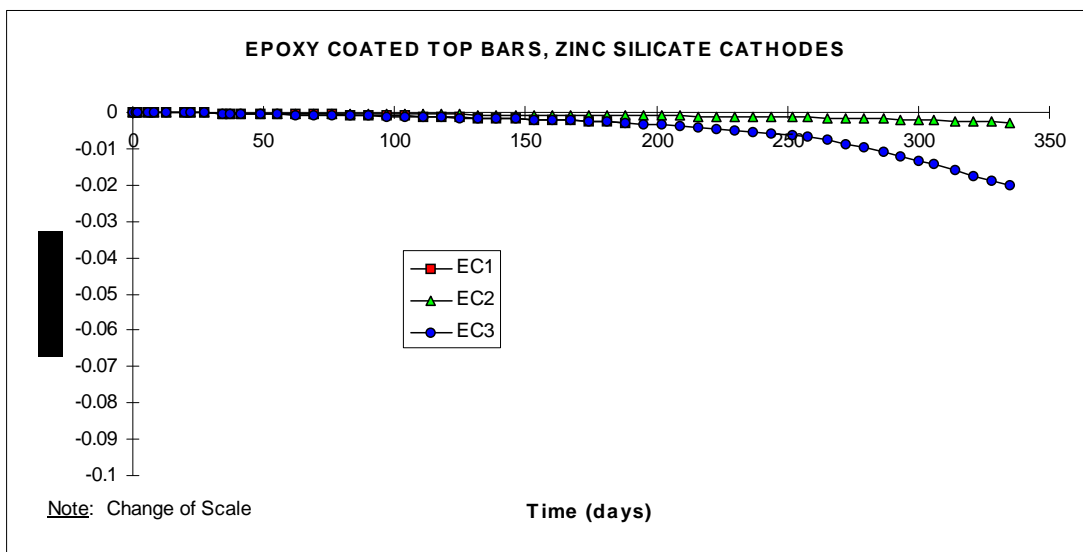


Figure 5.18: Cumulative Charge Flow/Damage: Group 9

5.3.2 Analysis of Charge Flow Data

High Ratio Zinc Silicate-Coated Anodes: The charge flow plots in Figures 5.10-5.15 indicate that more corrosion took place in the macrocells using uncoated cathodes than the cells with coated cathodes. The specimens with coated cathodes are described in Figures 5.11, 5.13, and 5.15, with average total charge values of -1.9 kC, -1.6 kC, and -2.4 kC. The uncoated specimens gave average values of -5.4 kC, -4.7 kC, and -6.2 kC. Based on the total charge flow, the specimens with uncoated bottom steel may have experienced about 2.8 times the corrosion damage of the specimens with coated bottom steel. The specimens with uncoated cathodes appeared to corrode at increasing rates, while the corrosion rates of the coated cathode specimens remained comparatively constant, as indicated by the curved shape of the uncoated specimen charge flux curves; compared with the more linear curves from those with coated cathodes. Visual inspection confirmed this trend. The difference in degree of corrosion of the coated cathode specimens and the uncoated cathode specimens was greater at 13 months than at 7 months.

Epoxy-Coated Anodes: Figure 5.16 describes the macrocells with epoxy-coated anodes and high ratio zinc silicate-coated cathodes. The average total charge flow value for this group of specimens is -0.012 kC, approximately 100 times lower than the zinc silicate specimens with coated cathodes. The epoxy specimens showed no significant corrosion. However, the plot for specimen EC3 began to increase rapidly after 250 days of exposure, indicating an increasing corrosion rate.

Galvanized Anodes: The galvanized samples showed the same corrosion patterns as the high ratio zinc specimens. The cells with coated cathodes showed lower predicted damage and fairly constant corrosion rates, while the cells with uncoated cathodes showed higher values of charge flux and increasing corrosion

rates. The galvanized/coated cathode specimens had an average of -0.38 kC of charge flow, and the galvanized/uncoated cathode specimens an average of -3.4 kC. Both of these averages were substantially lower than the averages from the high ratio zinc silicate specimens. Based on charge flow, the galvanized would appear to have corroded less than the zinc silicate samples, however this was not found to be the case on inspection.

Irregular corrosion current activity following approximately 260 days of exposure is evident on the plots. Positive corrosion currents caused the graphs for specimens GB2, GC1, and GC2 to fluctuate and curve upward, indicating a shifting of the anode/cathode relationship. As mentioned, it appeared as if anodic dissolution was taking place on the bottom steel. On further inspection, a small amount of corrosion was found on the cathode steel within the concrete.

Summary: Comparison of Damage Predictions: The damage predictions have been summarized below in Table 5.1 for the specimens removed after 13 months. The macrocells have been listed in order of increasing damage, as predicted by charge flux. It is evident from Table 5.1 that both the epoxy and galvanized specimens were expected to show less damage than the corresponding high ratio zinc silicate specimens. Within the zinc silicates, the bars that were grit-blasted and repaired were predicted to see the most corrosion.

MACROCELL	DESCRIPTION	CHARGE FLOW (kC)
EC3	Epoxy-Coated Anodes; Coated Cathodes	-0.020
GC2	Galvanized Anodes; Coated Cathodes	-.11
WC2	Wire-Brushed and Repaired Anodes; Coated Cathodes	-1.8
NC3	Unrepaired Anodes; Coated Cathodes	-2.1
SC1	Grit-Blasted and Repaired Cathodes; Coated Anodes	-2.8
GB1	Galvanized Anodes; Uncoated Cathodes	-4.6
WB2	Wire-Brushed and Repaired Anodes; Uncoated Cathodes	-5.9
NB3	Unrepaired Anodes; Uncoated Cathodes	-7.1
SB3	Grit-Blasted and Repaired Anodes; Uncoated Cathodes	-7.7

Table 5.1: Summary of Total Charge Flux Values in Order of Increasing Damage Prediction

5.4 Inspection After Seven Months of Exposure

5.4.1 Corrosion Locations

In the case of all the high ratio zinc silicate specimens, corrosion was concentrated primarily in a zone extending 3 inches from the front faces of the macrocells. Corrosion was not specific to the resistor or non-resistor side, with three of the six samples showing more corrosion on the bar leg without the connection to the cathode steel. In earlier tests, ^[12] and in the galvanized specimens, corrosion was concentrated around the bend on the resistor side of the bars, reflecting a distance effect and macrocell action. The same mechanism did not appear to be present in these tests with the zinc silicate specimens. Very little widespread corrosion was observed

Figure 5.19: Corrosion Locations Typical of High Ratio Zinc Silicate Specimens

around the bends of the bars. Corrosion was the most severe near the front face, and in areas where voids in the concrete came into contact with the bars. Severe attack was observed in some cases at these void locations. Figure 5.19 gives an example of the corrosion found on the high ratio zinc silicate specimens.

The shifting of corrosion from the bends to the front-face locations indicates that another corrosion mechanism may be operating on the second-generation zinc silicate specimens. The corrosion was concentrated in the areas highest in oxygen content, both in the specimens with uncoated cathodes and in the specimens with zinc silicate-coated cathodes. Oxygen affects corrosion primarily through the cathodic reaction, suggesting that both anodic and cathodic reactions were taking place on the top steel coated with the high ratio zinc silicate. Microcell corrosion might therefore be the governing mechanism with the new zinc silicate specimens. In earlier tests, macrocell corrosion was observed to dominate.

5.4.2 Coating Adhesion to Concrete

The high ratio zinc silicate coating was found to adhere slightly to the concrete in the macrocells. In all of the specimens opened, some of the coating was observed to stick to the surrounding concrete when the bars were removed. Figures 5.20 and 5.29 show zinc silicate coating that has pulled away from the steel. The coating tended to pull away from around the bar deformations, leaving behind a thin gray residue on the bars. More coating pulled away from the zinc silicate bars that had been repaired than from the bars that were left unrepaired. The repaired bars had a thicker coating, permitting more zinc silicate to adhere to the concrete.

The concrete-to-coating adhesion was not as severe as with the previous generation of high ratio zinc silicate. Concrete adhesion seemed to be a critical factor in the failure of the earlier coating, and it was therefore a goal in the development of the second-generation zinc silicate to obtain a coating that did not

demonstrate such adhesion problems. Coating adhesion has not been eliminated in the current generation of coatings, but improvements have been made. Figure 5.20, below, illustrates the coating adhesion to the concrete observed after 7 months of exposure.

Figure 5.20: Adhesion of High Ratio Zinc Silicate Coating to Surrounding Concrete

In figure 5.20, the concrete immediately adjacent to the high ratio zinc silicate coated bars was significantly darker than the surrounding material. A close examination of the concrete revealed a sponge-like texture and pin-hole sized voids along the concrete/steel interface. The change in color and the presence of voids suggests that chemical reactions between the coating and the moist concrete may have produced gas bubbles and the observed discoloration.

5.4.3 Comparison of Corrosion Behavior

The most significant differences in the high ratio zinc silicate specimens were between the cells with coated and uncoated bottom steel. There was less corrosion on the specimens with zinc silicate-coated bottom steel than on the specimens with uncoated bottom steel. The charge flux data gave similar results. Figures 5.21 and 5.22, show the zinc silicate-coated steel with coated and uncoated cathodes examined in the 7-month autopsy.

Figure 5.21: High Ratio Zinc Silicate Anodes with Uncoated Bottom Steel

Figure 5.22: High Ratio Zinc Silicate Anodes with Coated Bottom Steel

Figures 5.22 and 5.23 show the high ratio bars, and illustrate the further point that, after seven months of exposure, the state of the zinc silicate coating prior to concrete placement did not significantly affect corrosion performance. There were only small differences between the unrepaired bars and the bars that were recoated, or between the bars repaired by different techniques. The only significant differences resulted from coating the cathodes. Galvanic action did take place with the zinc silicate coatings. Without galvanic protection the more heavily damaged anodes would have shown more corrosion than the bars with repaired coatings.

It was also observed that the galvanized specimens showed significantly more corrosion than the corresponding high ratio zinc silicate specimens. This result was surprising, as the charge flux data indicated lower currents with the

galvanized specimens than with any of the zinc silicate specimens with similar cathodes.

Figures 5.23 and 5.24 show the results with the galvanized and zinc silicate anodes. Corrosion of the galvanized bars was more widespread than on the bars coated with high ratio zinc silicate, and was located primarily around the bends, where the steel had yielded. Corrosion of the zinc silicate bars was located on the bar legs, near the face of the macrocells. As mentioned, it is possible the galvanized specimens experienced primarily macrocell corrosion, while the zinc silicate specimens experienced microcell corrosion. Regardless of the mechanism, though, the galvanized specimens did not perform nearly as well as the zinc silicate specimens.

**Figure 5.23: Comparison Between Galvanized
And Zinc Silicate Anodes**

Figure 5.24: Galvanized and High Ratio Zinc Silicate Anodes

Figure 5.25: Epoxy-Coated Anode

Figure 5.25 shows the epoxy-coated anode after removal from the macrocell. There was no visible corrosion on the bar, which appeared to be in pristine

condition. The epoxy specimen demonstrated the least corrosion of all the specimens opened. This behavior was reflected accurately by the charge flux data.

5.5 Inspection After Thirteen Months of Exposure

5.5.1 Corrosion Locations

Consistent with the 7-month autopsy, the high ratio zinc specimens opened after 13 months all showed corrosion in the first 1-3 inches from the front face of the macrocells. The additional vapor barrier applied after 8 months of exposure did not appear to halt corrosion in this area. No definite preference was shown for the resistor or the non-resistor sides of the bars. This corrosion damage again indicated microcell action, governed by the higher levels of oxygen near the face of the cells where the bars protruded.

The galvanized specimens did not show similar patterns of corrosion. The most severe corrosion was around the bends of the bars. The galvanized bar corrosion was more uniform and widespread over the bar surface area, indicating macrocell behavior.

Severe, localized corrosion was observed in both the high ratio and the galvanized specimens in locations where voids in the concrete contacted the bar surface. For example, sample WB2 showed an isolated area of corrosion at a void, even though the surrounding coating was in very good condition and should have been controlled by sacrificial action. Severe local exposure appeared to overwhelm the galvanic capabilities of the coating in this instance. In contrast, there were other voids along the same bar that produced no corrosion. A high chloride concrete environment therefore appears to be able to limit the local effectiveness of galvanic

action under some conditions - even when galvanic action in a global sense is taking place.

In addition, the high ratio specimens demonstrated a slight tendency to corrode more on the underside of the anode bars than on the top surfaces. In every instance where there was a significant difference in corrosion between the top and bottom of the bar, the bottom was more heavily corroded. This pattern was observed in 4 of the 6 high ratio specimens. All three specimens with uncoated cathodes were in this group. Figures 5.26 and 5.27 illustrate the higher levels of corrosion on the underside of the bars.

Figure 5.26: Corrosion: Top Surface of NB3

Figure 5.27: Corrosion: Bottom Surface of NB3

In contrast, the galvanized specimens were seen to corrode most severely on the top surfaces of the bars. Higher levels of corrosion in the galvanized specimens caused the concrete to crack, bringing more oxygen into contact with the tops of the anodes. It is expected that this crack-driven corrosion caused the galvanized bars to corrode more heavily on the top surfaces. Figure 5.28 shows the pattern of galvanized bar corrosion.

Figure 5.28: Galvanized Bar Corrosion

5.5.2 Coating Adhesion to Concrete

A particular point of interest in reference to coating adhesion was the question of behavior over time, i.e., whether the bond of the coating to the high ratio coated steel would change as a result of chemical reactions between the coating and concrete environment. No consistent pattern of changes in adhesion and coating delamination were observed. In one case, more of the coating adhered to the concrete after 13 months than after 7, while in another case, less adhesion was observed after 13 months. In other cases, no differences were observed. It was therefore concluded that differences in coating adhesion resulted from initial surface preparation and coating thickness, and were not induced by reaction with the concrete.

The three methods of coating application, however, did produce different performance and loss coating. More coating was found to pull away from the wire-brushed and recoated steel upon removal from the concrete than with the grit-blasted and repaired samples. The lowest loss of coating was observed with the unrepaired specimens.

Again, these differences were attributed to surface preparation between coats. The grit-blasted steel was given an ideal surface preparation, while the wire-brushed steel was not prepared as well prior to application of the repair coat. Poorer second coat adhesion probably caused more of the coating on the wire-brushed surface to pull away from the bars when removed from the concrete. Very little coating loss was observed with the unrepaired specimens because far less of the coating was left on the bars.

However, the different adhesion and pull-off characteristics did not appear to affect corrosion performance. Corrosion was not generally observed in areas where the coating pulled away from the steel. Also, the wire-brushed specimens showed somewhat less corrosion than the grit-blasted specimens, even though more coating was observed to pull away from the wire-brushed bars. The bond of this high ratio zinc coating to the concrete was not felt to be a determining factor in corrosion behavior.

In all high ratio zinc silicate specimens, there were definite differences in adhesion between the top and bottom surfaces of the bars. The coating pulled away from the top surfaces of the steel more than from the bottom surfaces. The texture of the bottom surfaces was also crusty, with small fragments of concrete still attached to the coating, in contrast to the smoother texture of the top surfaces. Figures 5.29 and 5.30 illustrate these differences.

Figure 5.29: Adhesion to Top and Bottom Surfaces; Zinc Silicate

Figure 5.30: Difference in Texture - Top and Bottom Surfaces

It was felt the differences in adhesion and texture may have been due to chemical reactions between the coating and the fresh concrete that produced small amounts of gas. The gas might have become trapped against the underside of the bars, resulting in tiny air pockets and a weakening of the bond between the bar and the concrete. This phenomenon would explain the propensity for corrosion along the bottom surfaces of the steel, the lower adhesion, and the sponge-like texture of the concrete along the interface.

5.5.3 Comparison of Corrosion Behavior

As observed in the specimens inspected at 7 months, the specimens with coated cathodes performed better than the specimens with uncoated cathodes. In each group of macrocells, less corrosion was observed in the cells with coated

Figure 5.31: Corrosion with Coated and Uncoated Cathodes

bottom steel. NB3, for example, corroded more severely than the corresponding coated-cathode sample, NC3. Figure 5.31 shows a comparison between NB3 and NC3.

The differences produced by using the coated cathodes were more pronounced after 13 months than after 7 months. The increasing disparity was caused by the fact that very little deterioration took place in the high ratio coated-cathode specimens between 7 and 13 months. The coatings were essentially in the same condition. In fact, the unrepaired group (NC) showed slightly less corrosion at 364 days than at 196 days. Figure 5.32, below, illustrates this observation.

Figure 5.32: Corrosion of Unrepaired Bars at 196 and 364 Days

It was apparent, therefore, that the coated-cathode high ratio specimens were able to maintain good protection throughout 13 months of severe exposure. Virtually all corrosion of these samples was restricted to the front-face regions, and

was not severe. Protection was maintained around the bends and at voids in the concrete.

In contrast, the uncoated-cathode, high ratio zinc silicate specimens deteriorated significantly between 7 and 13 months. Corrosion spread from the front-face regions to the bends in the steel. Severe localized corrosion was also observed at concrete voids, although some voids did not produce corrosion. It is possible that the higher conductivity of the uncoated cathodes and resulting higher rates of corrosion depleted the zinc in the high ratio coatings, decreasing their galvanic protection capability. It is also possible that chlorides penetrated to the depth of the bottom steel, forcing the top steel coatings to sacrifice for both mats of steel. Clearly, the uncoated-cathode specimens showed signs of increasing distress.

The corrosion performance of all the high ratio specimens using coated cathodes was fairly uniform. Consistent with the 7-month inspection, the wire-brushed specimen showed slightly less corrosion than both the grit-blasted specimen and the unrepaired specimen, but the differences were slight. The high ratio zinc silicate specimens with coated cathodes all demonstrated essentially the same corrosion performance. It may be concluded, therefore, that when coated cathodes were used, the zinc silicate coatings were able to function galvanically for at least 13 months of exposure. During this time, damage levels to the coating induced by bending the bars did not significantly affect corrosion performance.

In contrast, coating damage impacted the corrosion performance of the high ratio samples with uncoated cathodes. While similar corrosion damage was found on samples SB3 and WB2, sample NB3 was corroded over a much larger area. Moderate corrosion was observed over a large portion of the underside of the bar. See Figure 5.27 for an illustration of corrosion to NB3. It is therefore evident that as the high ratio zinc silicate coatings depleted sacrificially, damage levels to the

coatings became significant. Clearly, it is important to repair coating damage where possible.

Both galvanized specimens opened after 13 months demonstrated much more corrosion than any of the high ratio zinc silicate bars. These specimens were also much more corroded than the galvanized specimens opened after 7 months. Corrosion appeared to have accelerated during this time period.

Figure 5.33: Galvanized Bars After 13 Months of Exposure

The galvanized steel was corroded over much of the bar surface area, with noticeable area reduction. Severe attack was observed near the site of cracks in the concrete. Figure 5.33 shows the galvanized bars. The photograph was taken after the black and green corrosion products changed to rust color.

The galvanized specimen with coated cathodes demonstrated less corrosion than the specimen with uncoated cathodes, but the difference was less pronounced than with the high ratio specimens. The use of coated cathodes in the galvanized cells did not retard corrosion to the same extent.

This behavior suggests a synergistic interaction between steel with the same coating. The high ratio zinc silicate coating prevented corrosion most effectively when all of the steel was coated with the high ratio coating. It may therefore be concluded that the high ratio zinc silicate coating should be used on all steel to provide maximum corrosion protection.

As in the 7-month autopsy, the epoxy specimen showed no visible signs of corrosion after 13 months of exposure. The epoxy coating consistently provided the best corrosion protection to the reinforcing steel out of the coatings investigated in this study. It must be underscored, however, that the epoxy was completely undamaged prior to concrete placement. Epoxy coatings provide exceptional protection when the coatings are free from defects. It may be difficult to achieve this standard in practice.

The high ratio zinc silicate coatings, on the other hand, demonstrated good corrosion protection and resilience to coating damage when the coatings were applied to all the steel in the concrete.

5.5.4 Reliability of Damage Predictions

A comparison was made between the corrosion damage predicted by total charge flux and the actual damage as observed visually after 13 months. For the visual inspection, a ranking of 10 was awarded to the most heavily damaged bar, and a ranking of 1 was awarded to the bar with the least observed corrosion. The remaining bars were ranked in order of relative damage. Damage was assessed according to corroded surface area and depth of penetration.

In terms of charge flux, a value of 10 was awarded to the specimen with the highest flux, and a 1 was awarded to the bar with the lowest flux. Linear interpolation between these two extremes was used to assign rankings to the remaining bars.

The results of the damage rankings are presented below, in Table 5.2.

MACROCELL	RATING BASED ON OBSERVED DAMAGE [10=WORST; 1=BEST]	RATING BASED ON DAMAGE PREDICTIONS [10=WORST; 1=BEST]
EC3	1	1
GC2	8	1.1
WC2	1.5	3.1
NC3	2	3.4
SC1	3	4.3
GB1	10	6.4
WB2	4	7.9
NB3	6	9.3
SB3	5	10

Table 5.2: Predicted and Observed Damage Rankings

It is evident from Table 5.2 that the charge flux readings failed to accurately predict the damage to the galvanized bars. The galvanized specimens were ranked second and sixth according to charge flux, although they were the two most severely corroded specimens opened in the autopsy. The potential measurements obviously failed to track the corrosion that was taking place in these macrocells.

Damage to the remaining bars was predicted more successfully. The order of rankings given by charge flux was identical to the order assigned by visual inspection, with one exception. Charge flux levels indicated greater damage to SB3 than to NB3, while observation showed NB3 to have a larger corroded surface area than SB3.

However, the numerical values assigned in the two rankings were different, even though the specimens were largely ranked in the same order. For example, the charge flux resulted in a ranking of 3.1 for specimen WC2, while visual observation assigned a ranking of 1.5. The charge flux values failed to identify the most extreme case of corrosion, so the relative scale for the charge flux was more compressed than it should have been.

It may therefore be concluded that corrosion potentials and charge flux calculations may be used to approximate the relative performance of high ratio zinc silicate coatings in a macrocell model. Charge flux accurately ranked the high ratio specimens, with one exception, and clearly illustrated the benefits of coating the bottom steel. Caution should be exercised in comparing corrosion flux data from different coatings, however, particularly when the coatings are galvanic.

5.6 Corrosion Products

The most prominent corrosion products visible on the zinc silicate samples were black. Small areas of dark green and rust-color were also observed. Upon exposure to the atmosphere, the black and dark green substances changed to rust-color within minutes. The fact that all of the products changed to rust-color indicates that iron was the primary material in the corrosion product.

Other research has found zinc to produce zinc oxide (ZnO), zinc hydroxychloride ($\text{ZnCl}_2 \cdot 4\text{Zn}(\text{OH})_2$), and zinc hydroxychloride II ($\text{Zn}_5(\text{OH})_8 \cdot \text{H}_2\text{O}$) during corrosion.^[13] Zinc oxide is white in color and could have been mistaken for fragments of concrete in the autopsy. Neither zinc hydroxychloride nor zinc hydroxychloride II were observed on the steel bars.

The black corrosion products were expected to be black magnetite (Fe_3O_4). Black magnetite is known to react with oxygen to form red brown iron (III) oxide, $2\text{Fe}_2\text{O}_3 \cdot \text{H}_2\text{O}$, accounting for the observed transformation to rust-color.

The dark green products appeared to be a complex chloride compound. Other researchers have observed dark green products to form during the chloride corrosion of steel in concrete, changing to rust-color upon exposure to the atmosphere.^[1] These phenomena correspond well with the behavior observed during autopsy.

5.7 Chloride Data

5.7.1 Autopsy Results

The chloride concentrations at a depth of 1-2 inches were measured prior to inspection for each macrocell opened. The results are given in Figures 5.34 and 5.35.

Examination of the figures yields several observations. For each autopsy, the chloride concentrations measured at the depth of the top reinforcing steel were fairly consistent. The readings taken after 196 days gave high and low chloride concentrations of 0.33% and 0.30%, with a mean value of 0.31% and a standard deviation that was 5.7% of the mean. The 364-day readings gave a high of 0.36%, a low of 0.28%, a mean value of 0.33%, and a standard deviation of 7.6% of the mean. These results show less variability than was anticipated.

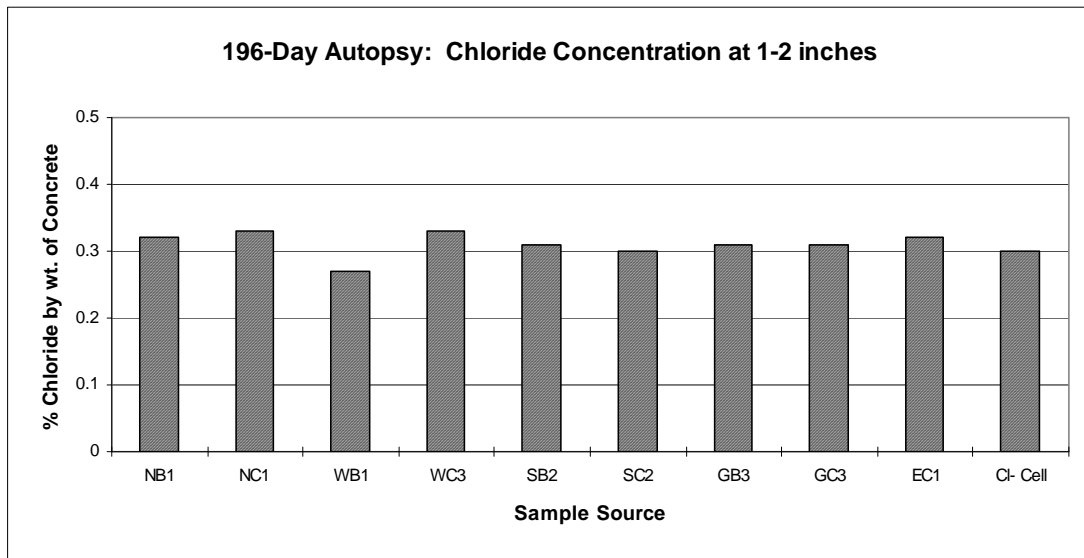


Figure 5.34: Chloride Concentrations after 196 Days of Exposure

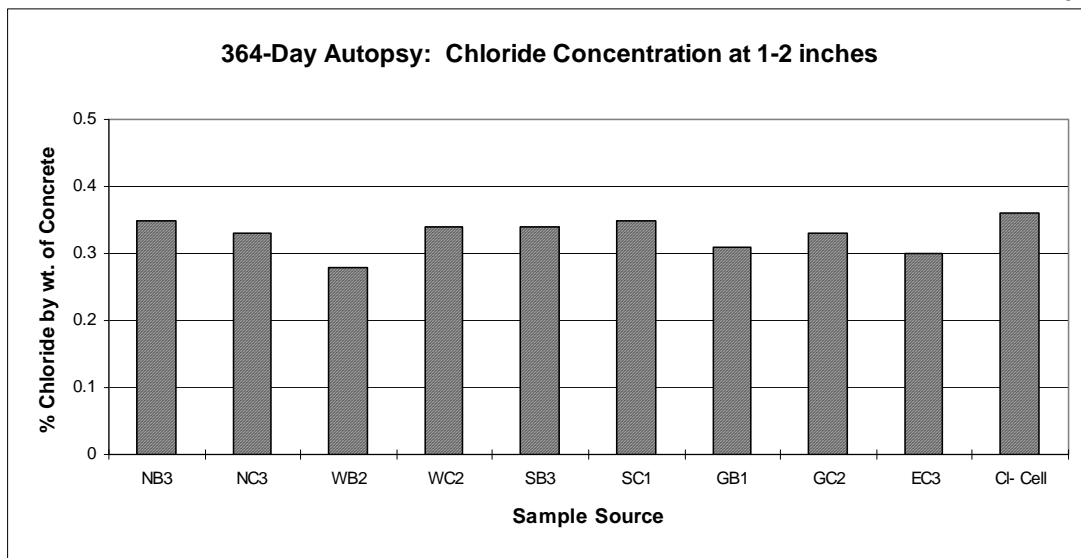


Figure 5.35: Chloride Concentrations after 364 Days of Exposure

The scatter observed was probably due for the most part to lack of homogeneity in the concrete. In addition, the depth range sampled was larger than recommended. The scatter would also be reduced if the number of samples taken from each specimen was increased.

Based on these results, the chloride measurements may be considered a consistent indicator of the chloride exposure conditions in concrete. However, the exposure conditions should not be used to predict levels of corrosion, particularly when corrosion protection systems are employed. No correlation was found between measured chloride concentration and the differences in corrosion performance of the specimens.

Finally, the average chloride concentrations at the depth of the top steel did not change significantly between 196 and 364 days of exposure. Over a period of six months, the mean chloride concentration increased from 0.31% to 0.33%. Exposure conditions therefore remained largely the same during that period.

5.7.2 Changes in Chloride Concentration Over Time

Figure 5.36, below, plots the chloride concentration measured at a depth of 1.375 inches from the exposed face of the chloride cells as a function of time.

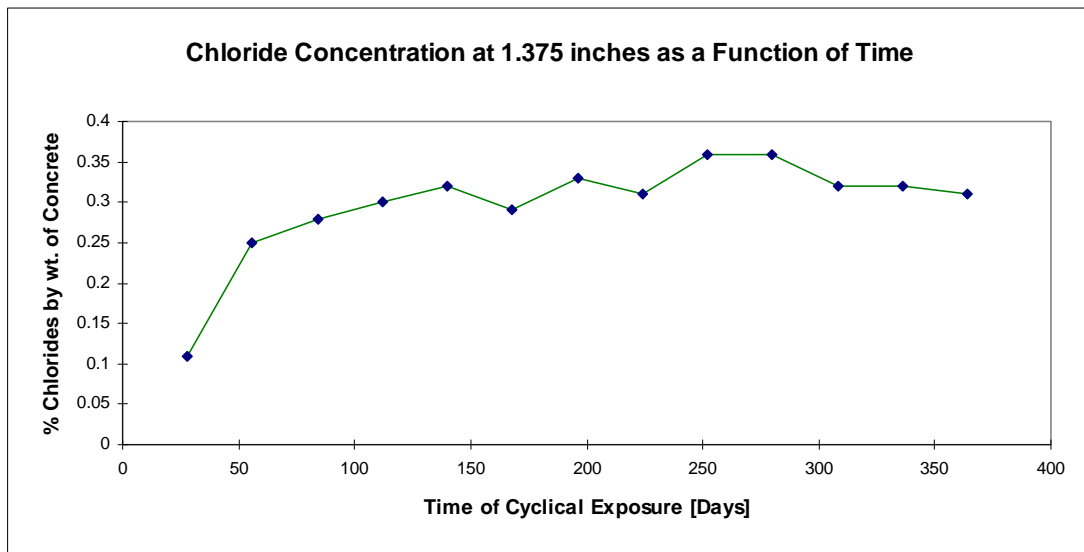


Figure 5.36: Chloride Concentrations at the Level of the Top Steel Over the Life of the Experiment

The above graph shows a sharp increase in chloride levels in the first month of exposure, followed by a more gradual, steady increase for the next three months. After the fourth exposure cycle, the gradual increase continued, but with a less consistent trend. The chloride levels appeared to reach an upper limit of approximately 0.35% by weight of concrete after about 250 days.

It is noteworthy that the chloride concentration at the level of the top steel reached 0.11% after only one exposure cycle. Chloride concentration guidelines suggest that corrosion initiates at chloride concentrations of approximately 0.05% by weight of concrete.^[22] The exposure conditions were therefore severe over virtually the entire life of the experiment.

Chloride concentration depth profiles obtained from the chloride samples at 3, 6, 9, and 12 months have been plotted on the same scale in Figure 5.37, below. The graphs show a maximum chloride concentration of approximately 0.4% by weight of concrete. This maximum was reached at a depth of .375 in. after the second exposure cycle, and over time, it was observed that greater depths approached, but did not exceed, this 0.4% limit.

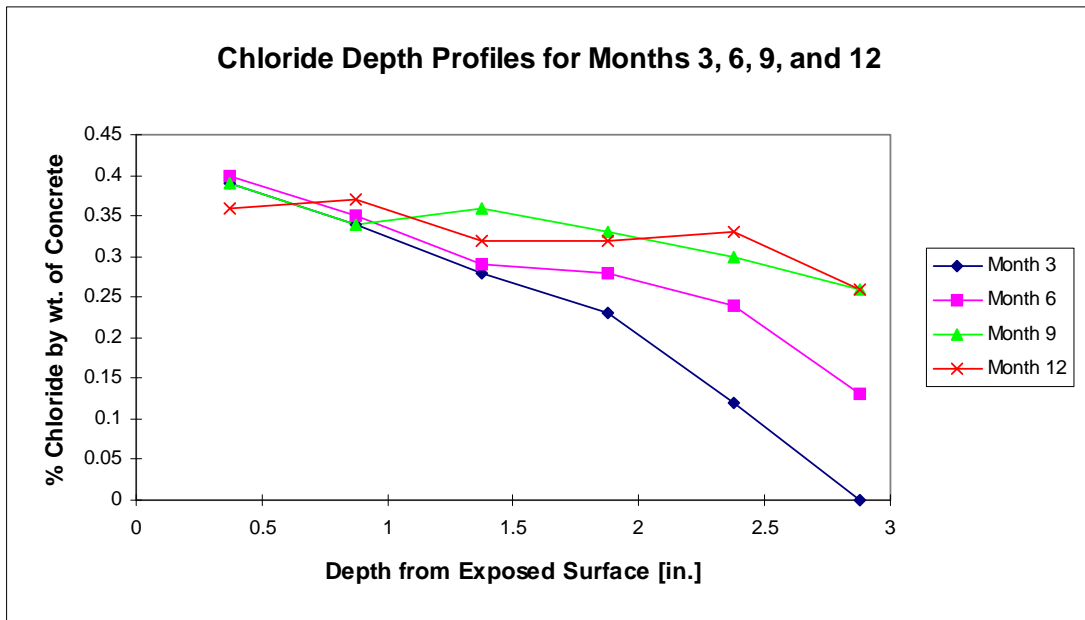


Figure 5.37: Chloride Depth Profiles Showing Chloride Diffusion Over Time

The 0.4% limit to the chloride concentration may be a function of the concentration of the solution used in ponding. Alternately, the limit may be a function of a chloride saturation level particular to the concrete mix used in this study.

CHAPTER 6

SUMMARY, CONCLUSIONS AND RECOMMENDATIONS

6.1 Summary

Twenty-seven macrocells, comprised of 9 groups of 3 cells each, were constructed for exposure testing. Six of the groups incorporated steel coated with a high ratio inorganic zinc silicate, two groups incorporated galvanized steel, and one group used epoxy-coated top steel. In three of the high ratio groups, uncoated bottom steel was used, and in the other three, bottom steel coated with the high ratio zinc silicate was used. Similarly, one galvanized group had uncoated bottom steel, while the other had high ratio-coated bottom steel. The macrocells in the epoxy group had high ratio-coated bottom steel.

Three coating and repair procedures were investigated with the high ratio zinc silicate specimens. Top steel that was not repaired following bending and transportation was used with two groups, top steel that was wire-brushed and repaired following bending was used in two groups, and top steel that was grit-blasted and repaired after bending was used in the remaining two groups. The three conditions tested the effects of different damage levels and repair techniques on the corrosion performance of the high ratio zinc silicate.

The macrocells were subjected to 13 cycles of chloride exposure (two weeks wet, and two weeks dry). Instantaneous electrical potential readings between the top and bottom mats of steel were taken at weekly intervals to measure corrosion currents, which were integrated over time to estimate total corrosion damage levels. Specimens were removed from exposure testing and the coated bars were inspected after 7 and 13 months of exposure to correlate visible corrosion damage with

current readings. Finally, the diffusion of chloride ions into the concrete was monitored at monthly intervals.

Corrosion current data and visual inspection produced the following results:

1. The macrocells with coated bottom steel experienced less corrosion activity than the cells with uncoated bottom steel. This was found to be true with both the high ratio zinc silicate and the galvanized specimens.
2. The high ratio zinc silicate specimens with coated bottom steel demonstrated only small levels of corrosion after 13 months, with minimal increases in visible corrosion damage between 7 and 13 months. Coating damage and repair techniques did not significantly affect observed corrosion performance.
3. The high ratio zinc silicate specimens with uncoated bottom steel showed light corrosion damage after 7 months, but deteriorated considerably between 7 and 13 months. Coating damage was found to affect corrosion performance, with more corrosion occurring on the unrepaired bars.
4. The wire-brushed and repaired zinc silicate bars produced slightly lower corrosion currents and demonstrated slightly less visible corrosion damage than the grit-blasted and repaired bars.
5. The second-generation high ratio zinc silicate coating was found to have different concrete adhesion characteristics than the first-generation that was tested in a similar fashion earlier. Although some adhesion and pull-off was observed with the second-generation, debonding was less severe and more localized than with the first-generation. Also, corrosion did not tend to occur in areas where the coating pulled away from the steel.
6. In the high ratio zinc silicate samples, a better bond to the concrete was observed along the top surfaces of the bars than along the bottom surfaces. Corrosion was often more severe on the bottom surfaces.

7. Corrosion current data erroneously predicted more corrosion damage in the high ratio zinc silicate specimens than in the galvanized specimens. It was found in the 7 and 13-month autopsies that the galvanized top bars corroded significantly more than the high ratio zinc silicate top bars.
8. The epoxy bars experienced no visible corrosion after 13 months of exposure.
9. Chloride concentration data revealed that consistent, severe exposure conditions were present for the final six months of testing. Chloride levels at the depth of the top steel were high enough to promote corrosion after only 2 months of exposure.

6.2 Conclusions

The test results allowed the following conclusions to be made:

1. The high ratio zinc silicate coating examined in this round of tests demonstrated superior corrosion performance to the high ratio zinc silicate formulation studied earlier. Less corrosion was observed on the steel protected with the new coating after 7 months of exposure, and corrosion damage was more localized. The new coating gave evidence of galvanic protection, preventing corrosion in areas of damage while zinc remained in the coating. The first generation coating did not appear to provide sacrificial protection.
2. The high ratio zinc silicate coating outperformed the galvanized coating investigated in these tests. Both the 7 and the 13-month inspections revealed more corrosion on the galvanized bars than on the corresponding high ratio bars. However, the condition of the galvanized bars prior to casting was poor, and may not have represented a state-of-the-art galvanized coating.

3. The epoxy coating provided the most effective corrosion protection of the coatings investigated. The epoxy coating was undamaged prior to casting. More corrosion might have occurred on the epoxy bars if the coating had been damaged, given the passive nature of epoxy coatings.
4. Coating adhesion/bonding to the concrete was not a dominant factor in the corrosion performance of the high ratio zinc silicate coating. No correlation was observed between areas where large amounts of the coating were removed from the steel when the concrete was demolished for inspection, and areas of corrosion damage.
5. The most significant factors governing the corrosion performance of the high ratio coating were oxygen levels, coating damage prior to casting, and the condition of the cathode steel. Corrosion was concentrated in areas rich in oxygen, and as corrosion progressed and the zinc in the coating became depleted, corrosion began to occur at locations of coating damage. Corrosion performance was dramatically improved by coating the cathode steel, in addition to the anode steel, with the high ratio zinc silicate. The high ratio zinc silicate coating provided good corrosion protection to the steel embedded in concrete when all the steel was coated in this fashion.

6.3 Recommendations

The following actions are recommended:

1. Conduct further tests, comparing the high ratio zinc silicate to state-of-the-art galvanized and epoxy coatings in a cracked-beam environment. The cracked-beam tests will simulate real-world conditions more accurately than the macrocells used in this series of tests, allowing for design life predictions. Damage levels representative of field conditions should be induced on all coatings prior to concrete placement. It is recommended that the cracked beams be subjected to chloride exposure in the laboratory and in a marine tidal zone.
2. Use the high ratio zinc silicate coating in test-case structures to begin long-term evaluation.
3. Continue to develop coatings with improved adhesion characteristics to the steel surface and long-term corrosion protection in concrete exposed to severe environments.

BIBLIOGRAPHY

1. "ACI Forum: Influence of Chlorides in Reinforced Concrete," Corrosion, Concrete, and Chlorides: Steel Corrosion in Concrete: Causes and Restraints. Detroit: American Concrete Institute, 1987.
2. Baker, E., Money, K., Sanborn, C. "Marine Corrosion Behavior of Bare and Metallic-Coated Steel Reinforcing Rods in Concrete," Chloride Corrosion of Steel in Concrete. Philadelphia: American Society for Testing and Materials, 1977.
3. Cady, P. "Corrosion of Reinforcing Steel in Concrete - A General Overview of the Problem," Chloride Corrosion of Steel in Concrete. Philadelphia: American Society for Testing and Materials, 1977.
4. Cook, A., Radtke, S. "Recent Research on Galvanized Steel for Reinforcement of Concrete," Chloride Corrosion of Steel in Concrete. Philadelphia: American Society for Testing and Materials, 1977.
5. Cook, H., McCoy, W. "Influence of Chloride in Reinforced Concrete," Chloride Corrosion of Steel in Concrete. Philadelphia: American Society for Testing and Materials, 1977.
6. Cornet, I., Bresler, B. "Corrosion of Steel and Galvanized Steel in Concrete," *Materials Protection*, April, 1966.
7. Delahunt, J., Nakachi, N. "Long Term Economic Protection with One-Coat of Inorganic Zinc-Rich," *Journal of Protective Coatings and Linings*, Vol. 6, no. 2, February, 1989.
8. Erlin, B., Hime, W. "Chloride-Induced Corrosion," Corrosion, Concrete, and Chlorides: Steel Corrosion in Concrete: Causes and Restraints. Detroit: American Concrete Institute, 1987.

9. Erlin, B., Hime, W. "Some Chemical and Physical Aspects of Phenomena Associated with Chloride-Induced Corrosion" Corrosion, Concrete, and Chlorides: Steel Corrosion in Concrete: Causes and Restraints. Detroit: American Concrete Institute, 1987.
10. Fontana, M. G. Corrosion Engineering. USA: McGraw Hill, Inc., 1986.
11. Fraczek, J. "A Review of Electrochemical Principles as Applied to Corrosion of Steel in a Concrete or Grout Environment," Corrosion, Concrete, and Chlorides: Steel Corrosion in Concrete: Causes and Restraints. Detroit: American Concrete Institute, 1987.
12. Frosch, R. "Performance of Reinforcing Steel Coated with a High Ratio Zinc Silicate," Master's Thesis. Austin: University of Texas at Austin, 1992.
13. Hime, W., Machin, M. "Performance Variances of Galvanized Steel in Mortar and Concrete," Corrosion Engineering, Vol. 49, No. 10, 1993.
14. Holm, J. "Comparison of the Corrosion Potential of Calcium Chloride and a Calcium Nitrate Based Non-Chloride Accelerator - A Macrocell Approach," Corrosion, Concrete, and Chlorides: Steel Corrosion in Concrete: Causes and Restraints. Detroit: American Concrete Institute, 1987.
15. Lehmann, J. "Cathodic Protection (Corrosion Control) of Reinforced Concrete Structures Using Conductive Coatings," Corrosion, Concrete, and Chlorides: Steel Corrosion in Concrete: Causes and Restraints. Detroit: American Concrete Institute, 1987.
16. McGlothlin, Q., Curtis, E., Cox, J. "Self-Curing Inorganic Zinc Coatings," Materials Protection, February, 1966.
17. Mehta, P. "Effect of Cement Composition on Corrosion of Reinforcing Steel in Concrete," Chloride Corrosion of Steel in Concrete. Philadelphia: American Society for Testing and Materials, 1977.
18. Munger, C. G. "Inorganic Zinc Coatings: A Review," Journal of Protective Coatings and Linings, June, 1987.

19. Munger, C. G. "VOC-Compliant Inorganic Zinc Coatings," *Materials Protection*, October, 1990.
20. Munger, C. G. Corrosion Prevention by Protective Coatings. Houston: National Association of Corrosion Engineers, 1984.
21. Munger, C. G. "Surfaces, Adhesion, Coatings," Anaheim, CA: National Association of Corrosion Engineers, Presented During *Corrosion/83*, 1983.
22. Peterson, C. G. "RCT Profile Grinding Kit for In-Situ Evaluation of the Chloride Diffusion Coefficient and the Remaining Service Life of a Reinforced Concrete Structure," Sweden: Presented at the *Chloride Ingress in Concrete Structures Symposium*, January, 1993.
23. Sanjurjo, S., Hettiarachchi, K., Wood, B., Cox, P. "Development of Metallic Coatings for Corrosion Protection of Steel Rebars," Washington: Strategic Highway Research Program, 1993.
24. Szokolik, A. "Evaluating Single-Coat, Inorganic Zinc Silicates for Oil and Gas Production Facilities in Marine Environments," *Journal of Protective Coatings and Linings*, March 1992.
25. Waldrip, H. "Testing Zinc-Rich Coatings for Protecting Steel," *Materials Protection*, May, 1966.
26. Weyers, R. and Cady, P. "Deterioration of Concrete Bridge Decks from Corrosion of Reinforcing Steel," *Concrete International*, Vol. 9, No. 1, January, 1987.
27. Yeomans, S., "A Conceptual Model for the Corrosion of Galvanized Steel Reinforcement in Concrete," Unofficial report released by the University College, University of New South Wales, Australia, 1993.

VITA

Jeffrey James Mitchell was born in Austin, Texas on August 5, 1970. He attended high school at The American School in London and The American School in Aberdeen, Scotland, where he graduated as Valedictorian in 1989. He began study at the University of Texas at Austin in the fall of 1989 for a Bachelor of Science in Engineering degree, and graduated in four years with honors. He began research at the Phil M. Ferguson Structural Laboratory, and entered the Graduate School of the University of Texas at Austin in Fall, 1993, where he studied for a Master of Science in Engineering degree. While in the Graduate School, he worked as a Research Assistant under Dr. James O. Jirsa, and twice received the Steadman Fellowship in Structural Engineering. He has also worked for three summers in the North Sea offshore oil industry.

Permanent Address: 1504 Ridgemont Dr.
 Austin, TX 78723

This thesis was typed by the author.